Journal of Human Evolution 55 (2008) 421–437

Contents lists available at ScienceDirect

Journal of Human Evolution

journal homepage: www.elsevier.com/locate/jhevol

A description of the Omo I postcranial skeleton, including newly discovered fossils

Osbjorn M. Pearson [a,*], Danielle F. Royer [b], Frederick E. Grine [c,d], John G. Fleagle [c]

[a] Department of Anthropology, MSC 01-1040, University of New Mexico, Albuquerque, NM 87131, USA
[b] Interdepartmental Doctoral Program in Anthropological Sciences, Stony Brook University, Stony Brook, NY 11794, USA
[c] Department of Anatomical Sciences, Stony Brook University, Stony Brook, NY 11794, USA
[d] Department of Anthropology, Stony Brook University, Stony Brook, NY 11794, USA

ARTICLE INFO

Article history:
Received 24 April 2007
Accepted 15 May 2008

Keywords:
Anatomically modern *Homo sapiens*
Omo Kibish
Middle Stone Age

ABSTRACT

Recent fieldwork in the Kibish Formation has expanded our knowledge of the geological, archaeological, and faunal context of the Omo I skeleton, the earliest known anatomically modern human. In the course of this fieldwork, several additional fragments of the skeleton were recovered: a middle manual phalanx, a distal manual phalanx, a right talus, a large and a small fragment of the left os coxae, a portion of the distal diaphysis of the right femur that conjoins with the distal epiphysis recovered in 1967, and a costal fragment. Some researchers have described the original postcranial fragments of Omo I as anatomically modern but have noted that a variety of aspects of the specimen's morphology depart from the usual anatomy of many recent populations. Reanalysis confirms this conclusion. Some of the unusual features in Omo I—a medially facing radial tuberosity, a laterally flaring facet on the talus for the lateral malleolus, and reduced dorsovolar curvature of the base of metacarpal I—are shared with Neandertals, some early modern humans from Skhul and Qafzeh, and some individuals from the European Gravettian, raising the possibility that Eurasian early modern humans inherited these features from an African predecessor rather than Neandertals. The fragment of the os coxae does not unambiguously diagnose Omo I's sex: the greater sciatic notch is intermediate in form, the acetabulum is large (male?), and a preauricular sulcus is present (female?). The preserved portion of the left humerus suggests that Omo I was quite tall, perhaps 178–182 cm, but the first metatarsal suggests a shorter stature of 162–173 cm. The morphology of the auricular surface of the os coxae suggests a young adult age.

Introduction

The initial discovery of the Omo I hominin skeleton was made in 1967 by a Kenyan team, led by Richard Leakey, of the International Palaeontological Research Expedition to the Omo Valley, southwestern Ethiopia (Leakey, 1969; Butzer, 1969; Butzer and Thurber, 1969; Day, 1969). The specimens came from near the top of Member I of the Kibish Formation, at the KHS (Kamoya's Hominid Site) locality. The Omo I remains were first described by Day (1969), who provided a preliminary description of the cranium and listed the associated postcranial elements recovered during that expedition. No morphological description of the postcrania was provided at that time, other than the observation that they appeared to be anatomically modern. In 1991, Day and colleagues published a more thorough anatomical description focused on the Omo I postcranial remains, along with limited metric analyses and comparisons. While the cranial remains of Omo I (and Omo II) have continued to figure prominently in debates on modern human origins, the Omo I postcranial material has rarely been incorporated into comparative studies.

In 1999, 2001, 2002, and 2003, an international team of researchers returned to the Omo Valley to renew excavations in the Kibish Formation. The goal of this effort, the Kibish Paleoanthropological Project, was to resolve longstanding debates over the age and provenance of the Kibish hominids and to gather more information about the archaeological and faunal context of the Kibish material. Using photographs and maps from the 1967 Leakey-led expedition, the KHS locality was relocated and verified. Extensive surface collections, new excavations, and microstratigraphic studies (see Feibel, 2008) were conducted at the site. New specimens attributed to the Omo I skeleton were discovered at KHS, including a fragment of right femur that conjoins with the distal femur discovered in 1967 (see Fig. 7).

* Corresponding author.
E-mail addresses: ompear@unm.edu (O.M. Pearson), danielle.royer@sunysb.edu (D.F. Royer), frederick.grine@sunysb.edu (F.E. Grine), john.fleagle@sunysb.edu (J.G. Fleagle).

0047-2484/$ – see front matter © 2008 Elsevier Ltd. All rights reserved.
doi:10.1016/j.jhevol.2008.05.018

From geological studies conducted during the recent expeditions, McDougall et al. (2005; see also Brown and Fuller, 2008; McDougall et al., 2008) were able to establish a more secure age framework for the Omo I fossils. Using $^{40}Ar/^{39}Ar$ dating of feldspars from tuffs in Members I and III of the Kibish Formation, they demonstrated that the KHS fossils must be older than 104 ± 1 ka, but younger than 196 ± 2 ka. Additionally, geological correlations to sapropel phases, the isotopic ages of pumice clasts in Member I, and evidence of the rapid deposition of Member I further narrow the age estimate to approximately 195 ± 5 ka for the Omo I fossils. Thus, the Omo I skeleton is currently the oldest well-dated anatomically modern human fossil.

The main goal of this paper is to present the results of a comprehensive study of all postcranial specimens attributed to the Omo I skeleton (Fig. 1), including details regarding the state of preservation, morphological description, and illustration. Furthermore, this paper provides a cross-referenced list of the various specimen numbers that have been applied to the skeleton in the decades since its initial discovery, noting instances of prior description, illustration, and analysis. In addition to the specimens that are described here, there are approximately 125 bone fragments that remain unidentified and that could not be refitted to another fragment. Day et al. (1991: 596) briefly described these as "approximately 800 grams of unidentified bone fragments" (our translation).

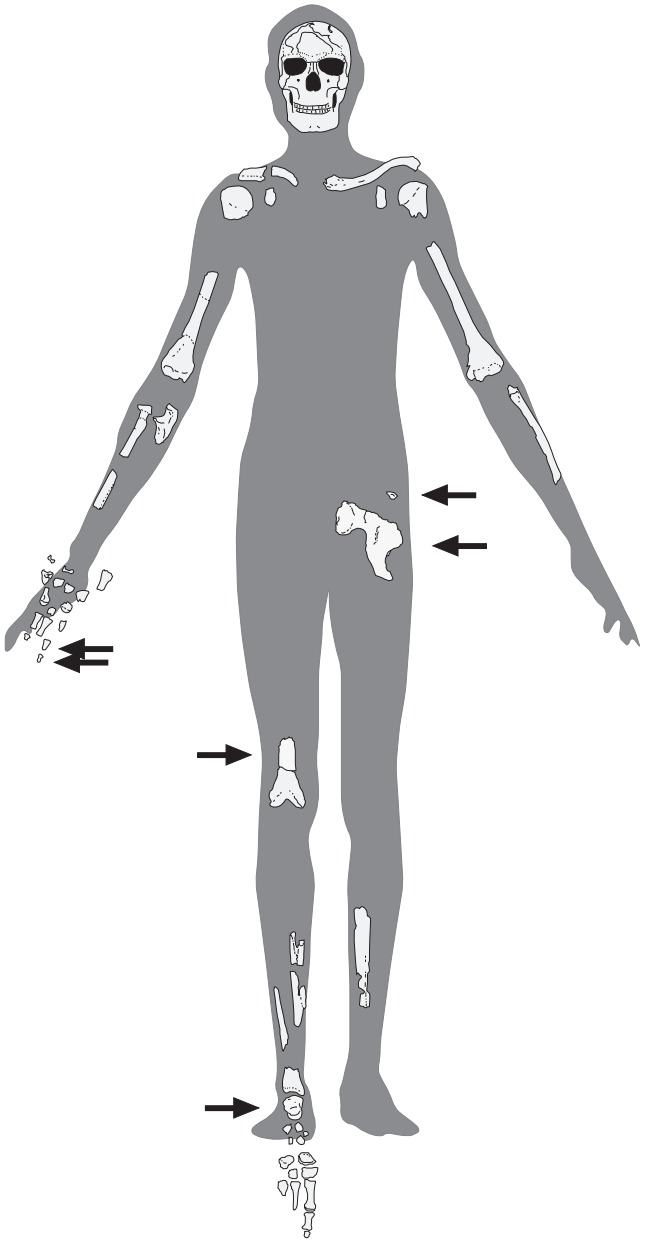

Fig. 1. The Omo I partial skeleton. Arrows indicate the newly recovered specimens. An outline of a Dinka man figured by Roberts and Bainbridge (1963) surrounds the bones.

Geological context

The Omo I skeleton was initially discovered by Kamoya Kimeu as a surface find near the base of a small hill in extensively dissected terrain on the east side of the Omo River. Following the collection of material on the surface, a step trench was dug into the hill and it was determined that the fossils had come from a single level in the upper part of Member I of the Kibish Formation (Butzer, 1969; see also Feibel, 2008). A laterally extensive excavation was made at this level that resulted in the in situ recovery of a few faunal remains, some stone tools, and a few skeletal elements of Omo I (Leakey, 1969; Clark, 1988). The additional parts of the skeleton that were recovered in the recent fieldwork were all found on either the deflated and eroded surface of the main excavation level from 1967 or on the eroded slopes within a few meters below that level. In addition, paleontological collecting indicated that all of the mammalian fossils in the immediate vicinity of this hill appear to be eroding from this same level.

As is evident from the following descriptions and illustrations, the Omo I skeletal fossils preserve many parts of both the appendicular and axial skeleton, but in a very fragmentary condition. Only the left clavicle, the right talus, the right first metacarpal, and a few other elements of the hand and foot are essentially complete. Most elements are extensively fractured and broken, but only a few show evidence of deformation or crushing, most notably the humeral heads. Some elements, especially the distal femur, show evidence of extensive postmortem abrasion. There are numerous pits and scratches on various elements.

Although no taphonomic analysis has been conducted on the Omo I fossils, all studies support the original interpretation that the interment of fossils was the result of normal geological processes. There is no evidence to support arguments that the presence of the Omo I fossils in Member I of the Kibish Formation was the result of an intrusive burial from a later time period (e.g., Klein, 1999). Likewise, given that no skeletal element is duplicated and that all appear to derive from an adult individual, the remains constituting Omo I almost certainly derive from a single associated skeleton.

Morphological description: upper limbs

Elements of the upper limb are relatively well represented in the Omo I individual. Most of the upper-limb specimens were collected during the 1967 Leakey-led expedition, although three new finds (a glenoid cavity fragment of the scapula, a manual middle phalanx, and a manual distal phalanx) were made during the course of recent fieldwork. The complete inventory of upper-limb remains is provided in Table 1.

Pectoral girdle

The pectoral girdle of Omo I consists of a nearly complete left clavicle, a fragment of the right clavicle, both scapular coracoid processes, and a fragment of the glenoid cavity of the right scapula (Fig. 2).

Specimen KHS 1-32 is a nearly complete left clavicle, lacking only the medial and acromial ends (Fig. 2a; see also Voisin, 2008). The clavicle displays some crushing of the inferior aspect of the lateral end of the shaft, while the acromial end of the shaft is

Table 1
Inventory of Omo I upper-limb specimens

Specimen number		Element	Side	Previous illustration	Notes
Omo 1967 KHS 1-#[a]	MN-#[b]				
2	20-A	Manual middle phalanx, ray III?	?Rt	Day et al., 1991 (Fig. 1)	
3	20-B	Manual middle phalanx, ray II	Rt	Day et al., 1991 (Fig. 1)	
9	12	Ulna, distal	Rt	Day et al., 1991 (Fig. 1)	
10	19-B	Manual proximal phalanx, ray III?, base	?Rt	No	
12	21	Metacarpal IV?, midshaft fragment	?	No	
16	16	Metacarpal I, head	Rt	Day et al., 1991 (Fig. 1)	
18	18	Metacarpal III, head and distal shaft	Rt	Day et al., 1991 (Fig. 1)	Listed as "metacarpal II" in Day et al., 1991: Table 1
19	33	Radius, proximal + diaphysis	Rt	Day et al., 1991 (Fig. 1)	
20	None	Metacarpal I, base	Rt	Possibly in Day et al., 1991 (Fig. 1)	
22	14	Lunate	Rt	Day et al., 1991 (Fig. 1)	
24	2	Coracoid process	Rt	Day et al., 1991 (Fig. 1)	
28	17	Metacarpal III, base + styloid process	Rt	Day et al., 1991 (Fig. 1)	
30	8	Humerus, diaphysis + distal epiphysis	Rt	Day et al., 1991 (Fig. 1)	
31	10	Humerus, diaphysis + distal epiphysis	Lt	Day et al., 1991 (Fig. 1)	
32	6	Clavicle	Lt	Day et al., 1991 (Fig. 1)	
33	7	Humerus, proximal	Rt	Day et al., 1991 (Fig. 1)	
34	9	Humerus, proximal	Lt	Day et al., 1991 (Fig. 1)	
36	20-C	Manual terminal phalanx, base (ray indet.)	?	No	
37	3	Coracoid process	Lt	Day et al., 1991 (Fig. 1)	
38	4	Clavicle, fragment	Rt	Day et al., 1991 (Fig. 1)	
39	11	Ulna, proximal	Rt	Day et al., 1991 (Fig. 1)	
40	13	Radius, diaphysis fragment	Rt	Day et al., 1991 (Fig. 1)	
41	15	Hamate, hamulus	Rt	Day et al., 1991 (Fig. 1)	
42	19-A	Manual proximal phalanx, ray IV?, head	?Rt	Possibly in Day et al., 1991 (Fig. 1)	
43	19-C	Manual distal phalanx, ray II? base	?Rt	Possibly in Day et al., 1991 (Fig. 1)	
48	34	Radius, diaphysis	Lt	Day et al., 1991 (Fig. 1)	
56	None	Glenoid fossa, scapula fragment	Rt	No	New find
57	None	Manual terminal phalanx, ray V?	?	No	New find
58	None	Manual middle phalanx, ray III	Lt	No	New find
None	5	Bovid rib fragment (contra Day et al., 1991)	–	Day et al., 1991 (Fig. 1)	Identified as "lateral Rt. clavicle frag." by Day et al., 1991

[a] Or revised here.
[b] Assigned by Day et al. (1991).

truncated at the oblique (trapezoid) line. There are large pits on the dorsal surface. Although the ends of the bone are missing, the clavicle is long, with a maximum length of 156 mm preserved. The intact specimen probably did not exceed 160 mm in length. The proximal portion of the shaft is strongly compressed superoinferiorly and elongated dorsoventrally, measuring 15 mm anteroposteriorly and 9 mm superoinferiorly at approximately the level of the specimen's midshaft. Approximately 10 mm lateral to the medial end, the shaft measures 26.6 mm dorsoventrally and 13.3 mm superoinferiorly. Laterally, the shaft displays torsion and is

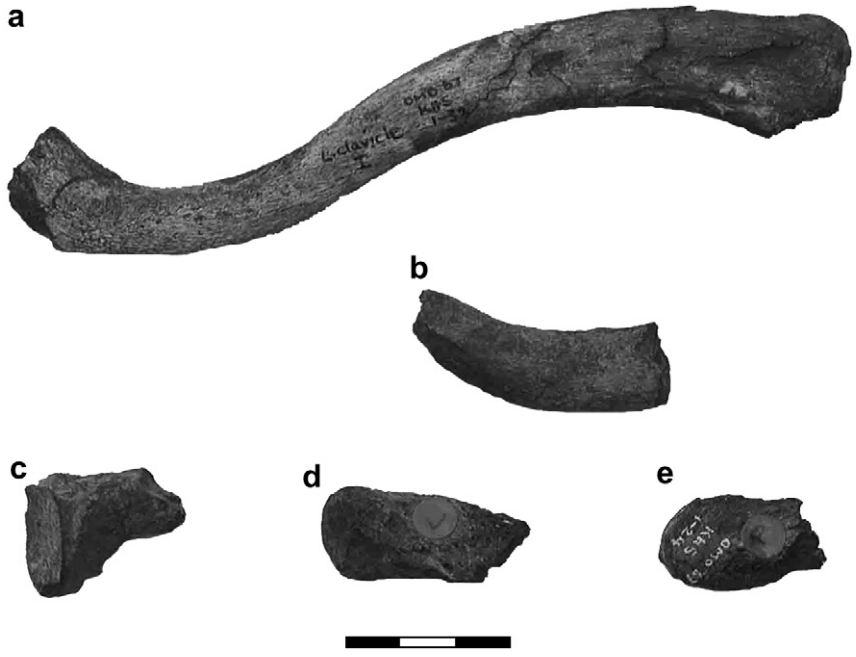

Fig. 2. Pectoral girdle: (a) left clavicle (KHS 1-32); (b) fragment of the right clavicle (KHS 1-38); (c) fragment of the right glenoid fossa (KHS 1-56); (d) right coracoid process (KHS 1-24); (e) left coracoid process (KHS 1-37). Scale bar = 3 cm.

much more slender and rounded in cross section. Lateral curvature of the bone is weak, while medial curvature is stronger. At the point of maximum incurvature medial to the acromial end, the shaft measures 12.5 mm dorsoventrally and 12.6 mm superoinferiorly. Also at this point, a ~22-mm-long rough, blunt crest marking the origin of the clavicular belly of the deltoid muscle is visible. The left clavicle exhibits very well-developed markings laterally for the coracoclavicular ligament. There is a shallow groove for the subclavius muscle. The conoid tubercle is well developed, which is contrary to the observation by Day et al. (1991: 596) that "there is no discrete conoid tubercle" (our translation). The inferior surface of the proximal portion of the shaft bears a large, well-defined impression for the costoclavicular ligament, measuring 27.2 mm mediolaterally and 14.3 mm anteroposteriorly.

The right clavicle is represented by a single fragment (KHS 1-38) measuring 50 mm in length, preserving the medial third of the shaft at the medial curvature, but lacking the expansion at the medial end of the element (Fig. 2b). The shaft has a slightly ovoid cross-sectional outline, measuring 15 mm anteroposteriorly and 12.5 mm superoinferiorly. The inferior aspect displays a shallow furrow for the subclavius muscle, as well as a roughened impression (costal tuberosity) for the costoclavicular ligament. A second heavily crushed fragment (MN 5 of Day et al., 1991), measuring 46 mm long and 25 mm wide, was reported by Day et al. (1991) as representing a lateral part of the right clavicular shaft (Fig. 2c). The smoothness of both surfaces of the fragment and the absence of a conoid tubercle suggest that this specimen represents a rib fragment from a medium- to large-sized bovid rather than a human clavicular fragment.

The scapulae are represented by a terminal fragment of the right coracoid process (KHS 1-24), a terminal fragment of the left coracoid process (KHS 1-37), and a fragment of the glenoid cavity from the right scapula (KHS 1-56). The right coracoid fragment (Fig. 2d) is 30 mm long, with a broad (18 mm) and flat (10 mm) distal end bearing a slightly convex inferior surface and a slightly curved superior surface. The left coracoid fragment (Fig. 2e) measures 38 mm in length, also with a broad (17 mm) and flat (8.5 mm) distal end. The fragment is mildly concave inferiorly and convex superiorly. There is slight loss of bone along the posterior margin of this specimen. The fragment of glenoid cavity (Fig. 2c) is small (20 mm high by 16 mm broad). It preserves the posterior part of the articular surface along with a ~26-mm-long segment of the axillary border, which is approximately 10 mm thick. A small portion of the anterior aspect of the axillary margin is also preserved.

Arm

Much of both humeri is preserved, including the right humeral head, the right distal humerus with a distal portion of the shaft, the left humeral head with the proximalmost shaft fragment, and the left distal humerus with most of the shaft.

The right humeral head (Fig. 3a), KHS 1-33, suffered anteroposterior crushing that obscures some of its morphology and distorts dimensions of the neck and proximal shaft. The specimen measures 52.9 mm superoinferiorly. The dorsal third of the head is abraded, exposing trabecular bone. Although distorted and crushed, both the greater and lesser tubercles appear to have been relatively large and projecting. The lesser tubercle bears small osteophytes along its medial edge. Periarticular arthritic osteophytes ring the undamaged ventral margin of the head; these are most strongly developed along the anterosuperior quadrant of the head's margin. The maximum width of the arthritic lipping surrounding the anterior aspect of the humeral head is 13.2 mm, with only about 2 mm of relief from the surrounding anterior surface of the proximal shaft. There are also a few small pits on the articular surface near the anteroinferior border of the head, which appear to be a taphonomic artifact rather than arthritic degeneration. A small piece of encrusting matrix adheres to the center of the head. Approximate measurements of the right humeral head are ca. 45.0 mm (maximum inferosuperior head diameter) and ca. 43.6 mm (maximum anteroposterior head diameter).

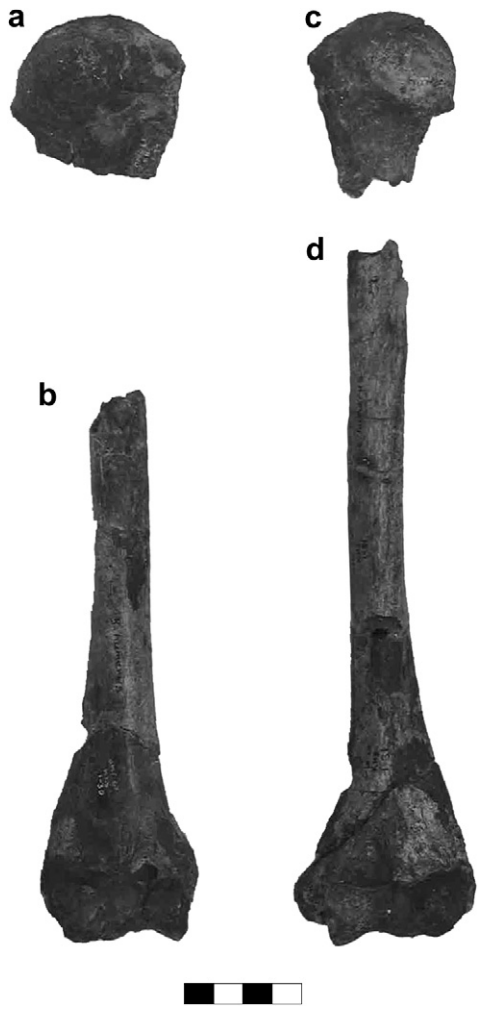

Fig. 3. Humeri (a) right humeral head (KHS 1-33) and (b) right humeral diaphysis and distal epiphysis (KHS 1-30), both in anterior view; (c) left humeral head (KHS 1-34) and (d) left humeral diaphysis and distal epiphysis (KHS 1-31), both in anterior view. Scale bar = 4 cm.

The remaining portion of the right humerus is represented by specimen KHS 1-30, a composite of four conjoining fragments with some small pieces of bone missing from each junction (Fig. 3b). The proximal portion of the shaft, including the deltoid tuberosity, is missing. The specimen is 187 mm in total length, while the shaft dimensions, measured 160 mm from the inferiormost point of the medial lip of the trochlea, are 21.0 mm (maximum diameter) and 19.3 mm (minimum diameter). The proximalmost portion of the preserved shaft is relatively slender. The diaphysis flares laterally as it joins the metaphysis, thereby providing a large surface for the origin of forearm musculature above the medial and lateral epicondyles. The attachment site for the origin of the extensor carpi radialis longus and brachioradialis muscles is clearly marked by a shallow sulcus measuring 15.4 mm superoinferiorly and 4.6 mm mediolaterally. The lateral epicondyle bears a large, rugose attachment site for the common extensor tendon. The medial epicondyle is heavily abraded. A septal aperture is present in the olecranon fossa, although a cast of the specimen made prior to full preparation suggests that the posterior margin of this aperture is irregular. Thus,

all or part of the aperture may be an artifact of preparation. The anteroinferior surface of the capitulum is eroded and trabecular bone is exposed. The anterior surface of the lateral aspect of the trochlea is also damaged, as is much of the medial lip of the trochlea. Slight osteophytic lipping is present around the margins of the elbow joint capsule, the lateral margin of the capitulum, and the lateral edge of the trochlea. As described below, the proximal right radial and ulnar fragments also bear extensive arthritic changes that corroborate the impression of an arthritic right elbow in the Omo I individual.

Figure 3c depicts specimen KHS 1-34, the head, neck, and proximalmost portion of the shaft of the left humerus. This specimen has suffered less crushing than the right humeral head, although the anterior third of the left head has been completely destroyed by abrasion. Based on what remains of the dorsal aspect of the head, it appears that the greater tubercle was well developed and projecting. The lateral surface of the greater tubercle bears several small osteophytes, while the superior third of the head's articular surface is slightly abraded (possibly from postmortem damage). No arthritic lipping is visible along the preserved margins of the left humeral head. The neck and shaft of the humerus are strongly concave posteriorly and medially below the head. The smooth attachment site for the insertion of teres minor faces inferiorly and posteromedially, whereas in modern humans it faces laterally.

The shaft and distal end of the left humerus, KHS 1-31, are shown in Fig. 3d. The specimen comprises eight principal fragments, with glue-filled gaps of 1–2 mm separating three of the fragments. The shaft dimensions, measured at nearly the same spot as on the right humeral shaft are 21.4 mm (maximum diameter) and 18.5 mm (minimum diameter). (Due to a large crack in the left shaft at 160 mm from the inferiormost point of the medial lip of the trochlea, the left shaft dimensions were measured at 152 mm from this point.) Thus, the degree of asymmetry in the dimensions of the Omo I humeral diaphyses appears to be fairly low, especially in comparison to the strongly asymmetric humeral diaphyses of Neandertals and many Upper Paleolithic European fossils (Trinkaus et al., 1994; Churchill and Formicola, 1997). The KHS 1-31 shaft preserves the inferior 50 mm of the deltoid tuberosity, which is clearly delineated as a low, roughened area, and the left medial epicondyle is also intact. There is no septal aperture present in the left humerus. Overall, the left humerus is morphologically similar to the right humerus, showing a dramatic flare in the mediolateral width of the metaphysis above the epicondyles. The lateral supracondylar ridge bears a distinct pit, measuring 19.9 mm superoinferiorly by 3.1 mm mediolaterally, for the origin of the tendon of the extensor carpi radialis longus and brachioradialis. Arthritic lipping of the distal articular margins is less developed on the left humerus than on the right. Anteriorly, there is a faint lip on the superior surface of the trochlea just below the coronoid fossa, as well as on the lateral lip of the trochlea, but the medial lip of the trochlea appears unaffected by arthritic degeneration. Proximal to the capitulum, on the anterior aspect of the bone, there is a distinct 6.0–6.5-mm broad groove that curves proximally from the medial aspect of the capitulum. This groove appears to be related to hyperflexion of the elbow, accommodating the radial head. A vestige of this groove is present on the right humerus.

Because the inferiormost extent of the deltoid tuberosity usually corresponds to the midshaft of a humerus, it is possible to estimate the original maximum length of Omo I's left humerus. The specimen measures 184.3 mm from the inferiormost point on the trochlea to the inferior margin of the deltoid tuberosity. Doubling this measurement produces an estimate of 368.6 mm for the original maximum length (Pearson, 2000a). This value is similar to the length of the humerus of some of the tallest early modern humans, such as Qafzeh 8 (375.5 mm for the right side), Grotte des Enfants 4 (368.5 mm for the right side), Barma Grande 2 (377 mm for the right side), Barma Grande 5 (353 mm for the left side), and Predmostí III (360 mm for the right side) (Matiegka, 1938; Pearson, 1997). The estimate of humeral length can be used to make a rough estimate of stature from Trotter's (1970; cited in Steele and Bramblett, 1988) formulae for African-American males and females. If the length is taken as 36.86 cm, these formulae produce estimates of 182.3 ± 4.43 cm and 178.2 ± 4.25 cm for an African-American male and female, respectively. However, Omo I may have had slightly different—probably more linear—body proportions than the average African-American and the distal margin of the deltoid tuberosity is located proximal to midshaft in some individuals, notably in Neandertals (Endo and Kimura 1970; Endo, 1971; Hambucken, 1993). The estimates of stature for Omo I should be regarded only as approximate, but they suggest that the individual was at least moderately tall, and perhaps markedly so.

Forearm

The specimen KHS 1-19 consists of a 95.1-mm-long fragment of the right radius, preserving the head, neck, radial tuberosity and proximal diaphysis assembled from several smaller fragments (Fig. 4). The lateral and inferior sides of the radial head are badly

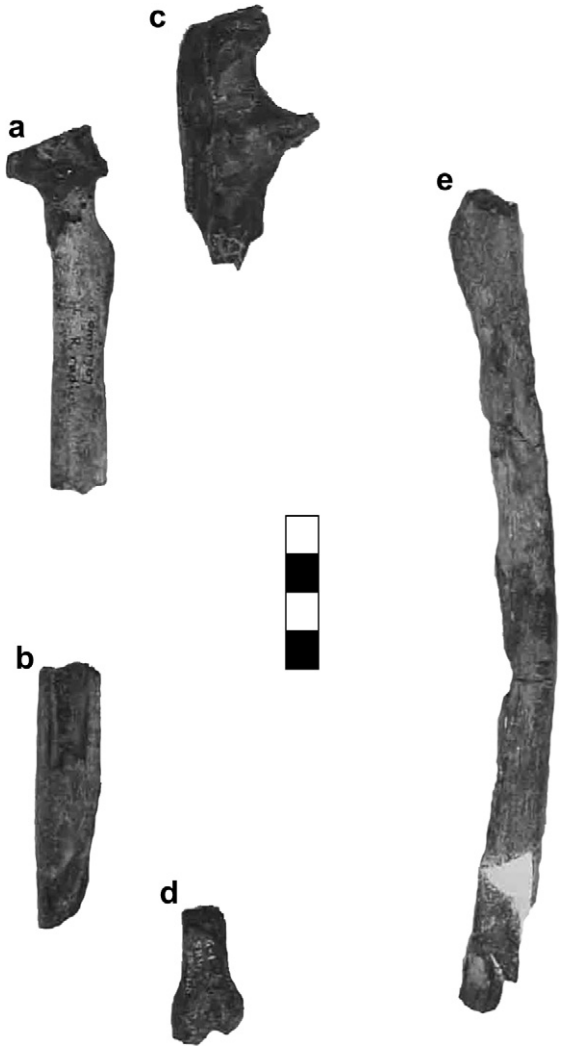

Fig. 4. Forearm: (a) right proximal radius (KHS 1-19); (b) right radial diaphyseal fragment (KHS 1-40); (c) right proximal ulna (KHS 1-39); (d) right distal ulna (KHS 1-9); (e) left radial diaphysis (KHS 1-48). Scale bar = 4 cm.

eroded, exposing cancellous bone. The radial head exhibits extensive arthritic modification; medially, it is pathologically thickened, reaching a maximum proximodistal dimension of 10 mm, and both the proximal and distal edges bear arthritic osteophytes. Osteophytes are also present along the medial aspect of the proximal rim, and they separate the anterior third of the head from the articular surface for the capitulum. The oblique line for the origin of the radial head of flexor digitorum superficialis is faintly visible, as noted by Day et al. (1991). The radial tuberosity is moderately developed. The interosseous crest intersects the radial tuberosity in its posterior third (position 2 of Trinkaus and Churchill, 1988), whereas it bisects the tuberosity in its middle third (position 3 of Trinkaus and Churchill, 1988) on the left radius. While a medial orientation of the radial tuberosity was once considered to be a common feature of Neandertals (Trinkaus and Churchill, 1988), it may simply be primitive for middle Pleistocene *Homo* since it occurs in both the 800,000-year-old ATD6-21 *Homo antecessor* radius from Atapuerca (Carretero et al., 1999) and in the late Early Stone Age (ESA) or Middle Stone Age (MSA) radius from Cave of Hearths, South Africa (Pearson and Grine, 1997).

Specimen KHS 1-40 is a 70-mm-long segment of the right radial diaphysis (Fig. 4). It bears no trace of the insertion for pronator teres, which typically lies at about the level of midshaft. The diaphysis is teardrop-shaped in cross section, with maximum and minimum diameters of 17.1 mm and 12.7 mm, respectively. The interosseous crest is nonprojecting, as on the left radius. The cortical bone appears to be thick based on the thickness at the proximal break: 6.0 mm laterally, 4.5 mm medially, 4.7 mm anteriorly, and approximately 4.1 mm posteriorly.

The left radius, KHS 1-48, is represented by a 212.5-mm-long segment of shaft, consisting of 10 conjoined pieces, that extends from the proximal edge of the radial tuberosity to the point at which the shaft begins to expand as the distal metaphysis (Fig. 4e). The specimen is moderately curved and very slender given its length, measuring a maximum of 14.3 mm in diameter and a minimum of 12.4 mm in diameter at the approximate level of midshaft (i.e., at the point of greatest lateral curvature). The interosseous crest is weakly developed, reaching its greatest development 70 mm distal to the edge of the radial tuberosity, where it projects only some 3.5 mm from the shaft. The interosseous crest bisects the tuberosity in its middle third (i.e., position 3 of Trinkaus and Churchill, 1988). The radial tuberosity is indistinctly delineated, measuring roughly 25.5 mm in proximodistal length and 15.2 mm in mediolateral width. The oblique line cannot be observed due to damage of the shaft inferolaterally to the radial tuberosity. There is an elongated, slightly roughened area (14.0 mm proximodistally by 5.4 mm dorsoventrally) for the insertion of pronator teres near the approximate level of midshaft.

Specimen KHS 1-39 is a fragment of the proximal end of the right ulna, preserving the olecranon process, trochlear notch, and coronoid process (Fig. 4). It is a relatively massive element, with a very broad olecranon process (26.3 mm in height by 25.9 mm in mediolateral diameter, excluding arthritic lipping medially). The coronoid process projects ventrally considerably more than the olecranon process, as is common in recent humans but not the MSA Klasies River Mouth and Border Cave ulnae (Churchill et al., 1996; Pearson and Grine, 1996) or the ~500-kyr-old Baringo Kapthurin ulna (Solan and Day, 1992). The coronoid process is much higher than in the Klasies specimen, but this may be slightly accentuated by the osteophytic lipping on the tip of Omo I's coronoid. The radial notch faces ventrally and is quite large, with a strong supinator crest extending down from it. A well-marked crest for the anconeus muscle is situated posterior to the supinator crest, as observed by Ward (1986). There is arthritic lipping around the lateral side of the olecranon, along the ventral margin of the entire coronoid process, and around the radial notch.

A small portion of the distal epiphysis of the right ulna is also preserved (Fig. 4d). The fragment KHS 1-9 consists of the head and styloid process; the overall size of this fragment seems quite small given the size of the proximal ulna. Erosion has damaged the ventral edge of the head. The tip of the styloid process bears a large arthritic pit ringed with osteophytic bone measuring ca. 5 mm in diameter.

Wrist and hand

The distalmost segment of the upper limb of the Omo I individual is represented by a mixed assortment of carpals, metacarpals, and phalanges, the majority of which are fragmentary and, with the exception of one newly discovered specimen and a few indeterminate elements, mostly come from the right side of the Omo I skeleton (Fig. 5).

Specimen KHS 1-22 is a nearly complete right lunate, showing only slight loss of periosteal bone along the medial margin (Fig. 5n). The element is extremely small and especially narrow, measuring 8 mm long proximodistally, 13.5 mm wide mediolaterally, and is 18 mm thick from dorsal to palmar aspect. There is a large, convex facet for the radius, a moderately broad nonarticular palmar surface, but virtually no dorsal nonarticular surface. The convex radial facet meets the concave capitate facet at its dorsodistal edge, but these two surfaces are separated by 3–4 mm of broken bone. There is a large, moon-shaped facet for the triquetral, but nearly no facet for the scaphoid.

Fig. 5m depicts specimen KHS 1-41, the hamulus of the right hamate, broken where it would have met the body. The specimen has a slightly concave radial aspect; it measures 11 mm tall, 11.5 mm wide proximodistally, and ca. 6.5 mm thick.

Specimen KHS 1-16 is the head of right metacarpal I. It was not listed in the Omo I postcranial inventory presented by Day (1969) or by Day et al. (1991: Table 1), although the fragment is possibly included in the upper-limb photograph in the latter publication (Fig. 1 in Day et al., 1991). Most of the articular surface of the head is preserved, measuring 14 mm wide and 14 mm deep (Fig. 5l). Also preserved is approximately 19 mm of the palmolateral aspect of the metacarpal shaft. There is a small tubercle on the medial side of the head for the first dorsal interosseous muscle. The base of the right metacarpal I, KHS 1-20, is also present (Fig. 5k). It retains a slightly saddle-shaped articular surface for the trapezium, and roughly 15.5 mm of the shaft. The dorsovolar contour of the base of Omo I's metacarpal I appears to be much less concave than those of many modern humans, a feature it shares with many Neandertals, some early modern humans from Skhul and Qafzeh (i.e., Skhul V and Qafzeh 9), and some individuals from the Gravettian culture of the European Upper Paleolithic, notably Grotte des Enfants 4 (Musgrave, 1971; Vlček, 1975; Trinkaus, 1983; Pearson, 1997). The base measures 17 mm dorsopalmarly and 17.5 mm wide. The dorsal surface is smooth and gently concave, while the palmar surface has a triangular cross section with a large, slightly concave ulnar face. A small (3×5 mm) osteophyte on the dorsolateral margin of the articular surface indicates some arthritic modification to the right palm.

The head and distal diaphysis of the right metacarpal III, specimen KHS 1-18, measures 30.5 mm in maximum length, preserving the articular aspect of the head together with some 17 mm of the shaft (Fig. 5h). The articular surface is convex and has an irregular outline, broader on the palmar than dorsal side. This results in an oblique path for the lateral margin of the articular surface. The ventral aspect of the head is 15 mm broad, the dorsal aspect is 9 mm broad, and the articular face is 5 mm deep dorsoventrally. This specimen was interpreted as a metacarpal II by Day et al. (1991). The base of the right metacarpal III is also present (Fig. 7j). Specimen KHS 1-26 consists of a styloid process, a saddle-shaped articular facet for the capitate, two separate (dorsal and ventral) facets for metacarpal IV medially, and a single narrow facet for

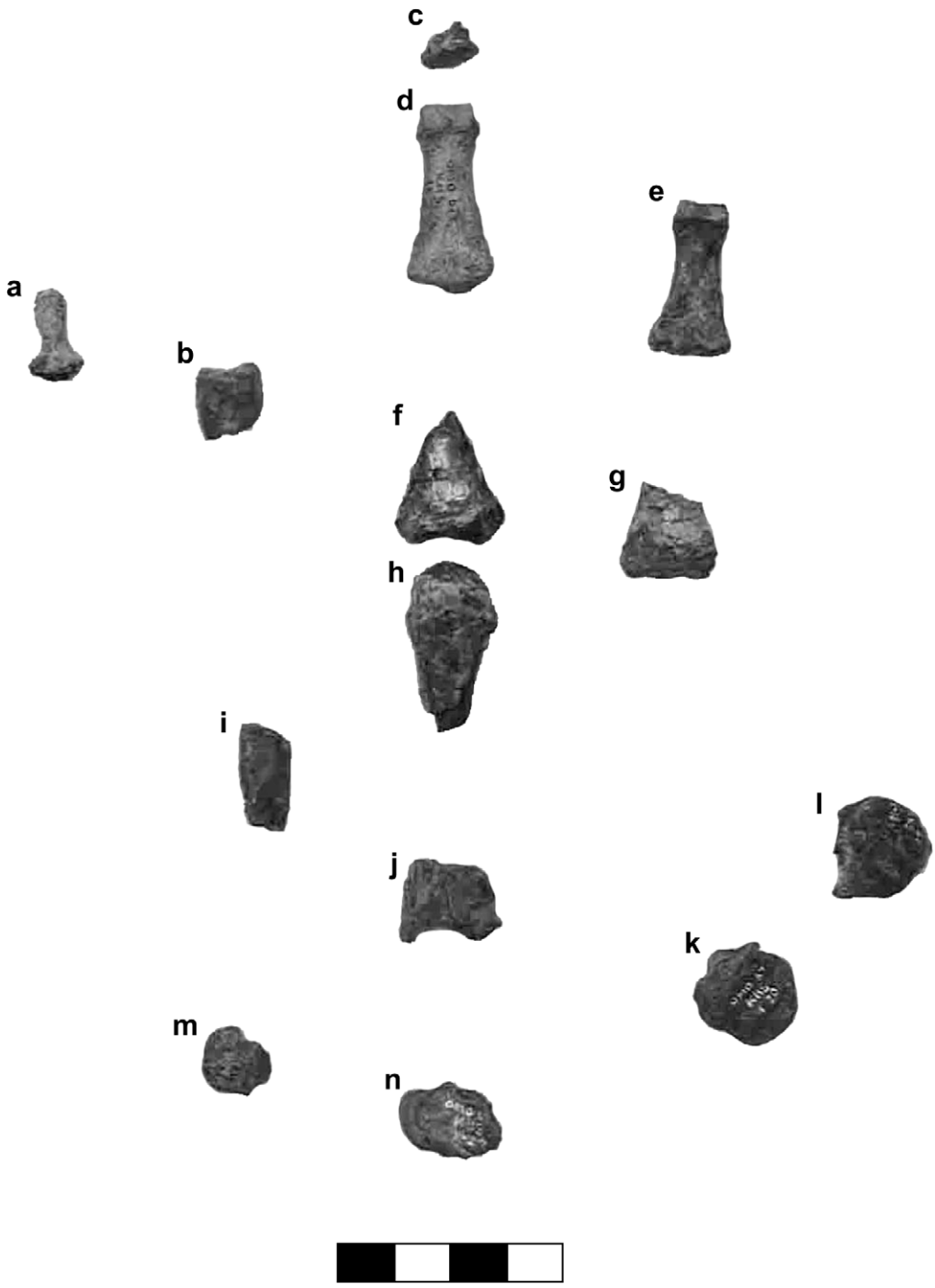

Fig. 5. Wrist and hand in palmar view except where noted: (a) newly discovered terminal manual phalanx, probably of ray V (KHS 1-57); (b) proximal phalanx head, possibly of ray IV (KHS 1-42); (c) base of a terminal manual phalanx, side and ray indeterminate (KHS 1-36); (d) middle manual phalanx, most likely of ray III (KHS 1-2); (e) middle manual phalanx from right ray II (KHS 1-3); (f) base of a proximal manual phalanx, probably of ray III (KHS 1-10); (g) base of a proximal phalanx, probably of ray II (KHS 1-43); (h) head of the right metacarpal III (KHS 1-18); (i) midshaft fragment, tentatively assigned to metacarpal IV (KHS 1-12); (j) base of the right metacarpal III (KHS 1-28); (k) base of the right metacarpal I (KHS 1-20); (l) head of the right metacarpal I (KHS 1-16); (m) hamulus of the right hamate (KHS 1-41) in lateral view; (n) right lunate (KHS 1-22). Scale bar = 4 cm.

metacarpal II laterally. The latter facet is continuous with the surface for the capitate, which measures 15.5 mm high and 8 mm broad. The styloid is well developed, with a deep pit adjacent to it at the margin of the articular surface for the capitate. The fragment also preserves about 13 mm of shaft.

Specimen KHS 1-12 is a fragment of the midshaft of a metacarpal (Fig. 5i). The fragment is short (19 mm) and narrow (8.5 mm mediolaterally by 10 mm dorsopalmarly), suggesting that it may derive from ray IV. Its side is indeterminate. This specimen was not illustrated by Day et al. (1991).

In their inventory of Omo I postcranial specimens, Day et al. (1991: Table 1) listed specimen MN 19 as a manual proximal phalanx head (KHS 1-42) plus two bases (KHS 1-10 and 1-43). Here, these fossils are treated as separate elements. Specimen KHS 1-42 is the head of a proximal manual phalanx, likely from the right ray IV (Fig. 5b). The fragment measures 13 mm in length and preserves the entire articular surface and a short segment of shaft. The head measures 12 mm mediolaterally by 8 mm dorsopalmarly. Specimen KHS 1-10 is the base of a manual proximal phalanx, likely from the right ray III (Fig. 5f). This fragment preserves the complete articular

surface and 23 mm of the ventral side of the shaft. Cortical bone is missing from the dorsal surface over the distal third of its preserved length, exposing an endocast of the medullary cavity. The articular surface is gently concave, measuring 14.7 mm mediolaterally and 11.2 mm dorsopalmarly. The base is 19 mm broad with nonarticular lips on the medial and lateral sides of the articular face. The dorsal aspect of the shaft is convex, while its palmar aspect is concave. Specimen KHS 1-43, the third element included by Day et al. (1991) in the MN 19 assemblage, is, as they suggested, interpreted here as the base of a manual phalanx, likely right ray II (Fig. 5g). The fragment preserves much of the proximal articular facet (the lateral side is missing) and 17 mm of the shaft, which is preserved mostly along the palmar aspect. The base measures 16.5 mm wide by 12 mm dorsopalmarly. The articular facet is very slightly concave. The dorsal aspect of the preserved shaft is convex, while its palmar surface is concave.

Day et al. (1991) included fragments KHS 1-2, 1-3, and 1-36 in an assemblage of manual phalanges that they designated as MN 20. A separate description of each fragment contained within this assemblage is provided here. Specimen KHS 1-3 is a complete middle manual phalanx from right ray II (Fig. 5e). The overall length of the element is 28 mm. The palmar surface has moderately elevated medial and lateral ridges for the attachment of flexor sheaths, and a roughened area between these ridges for the insertion of the flexor tendon. The dorsal aspect of the articular surface of the base has a slight bevel, which is indicative of arthritic degeneration. The maximum mediolateral diameter of the base is 14.5 mm, while the dorsopalmar diameter of the base is 9.0 mm. The head measures 9.5 mm mediolaterally by 6.0 mm dorsopalmarly, and the shaft waists to a mediolateral diameter of 7.5 mm and a dorsopalmar diameter of 4.5 mm. Specimen KHS 1-2 is a complete middle manual phalanx, regarded here as representing the right ray III (Fig. 5d). The maximum length of the bone is 32.5 mm; the base measures 15.5 mm mediolaterally by 9.5 mm dorsopalmarly. The head is 11.0 mm mediolaterally and 9.0 mm dorsopalmarly, while the shaft measures 8.0 mm mediolaterally by 5.0 mm dorsopalmarly. There are moderately developed ridges along both the medial and lateral margins of the shaft for the attachment of flexor sheaths, and these are better developed than on the left element. Specimen KHS 1-36 is here interpreted as the base of a terminal phalanx, and is discussed below.

A newly recovered complete middle manual phalanx from left ray III (KHS 1-58) was discovered during recent fieldwork. The shaft has suffered some damage immediately proximal to the expansion for the head (the bone is fractured at this point). The maximum length of the element is 31.5 mm. The base measures 14.5 mm mediolaterally by 9.5 mm dorsopalmarly. The head is 10.5 mm mediolaterally by 6.0 mm dorsopalmarly, with the articular width of the head measuring 8.5 mm mediolaterally. The shaft is 8.5 mm mediolaterally by 5.0 mm dorsopalmarly. There are slight ridges along the medial and lateral margins of the shaft for attachment of the flexor sheaths; however, these are better developed on the right element rather than on the left.

The specimen KHS 1-36 (Fig. 5c) is interpreted as the base of a manual terminal phalanx, with ray position and side indeterminate. The specimen measures 10.3 mm in total length. The articular facet is fairly flat, with distinct palmar and dorsal lips; it measures 9.0 mm mediolaterally by 6.5 mm dorsopalmarly. There are prominent tubercles medial and lateral to the facet. The proximal portion of the shaft has a roughened pit for the insertion of flexor digitorum profundus. The preserved shaft measures 5.5 mm mediolaterally by 4.0 mm dorsopalmarly.

Specimen KHS 1-57 is a newly discovered complete terminal manual phalanx, most likely deriving from ray V (Fig. 5a). The siding of this element is indeterminate. The specimen has suffered only slight damage to the margin of the apical tuft. The broad base preserves a small, oval facet with raised palmar and dorsal edges. The palmar surface of the shaft bears a roughened area for the attachment of the flexor digitorum profundus muscle. The shaft is waisted, with a notable distal expansion for the apical tuft. The element is 16 mm long, with a maximum mediolateral width of 9.5 mm. The articular surface measures ca. 7.5 mm mediolaterally, the apical tuft is 5.5 mm broad, and the shaft dimensions are ca. 4 mm mediolaterally by 3.8 mm dorsopalmarly.

Morphological description: lower limbs

The inventory of lower-limb remains from the Omo I skeleton has grown since the original Omo Kibish expedition, and now includes a large portion of the pelvis, a fragment of the femoral shaft that conjoins with the femoral distal epiphysis discovered in 1967, and a complete talus. As in the upper limbs, the majority of lower-limb elements are attributed to the right side, with the notable exception of the new os coxae fragments. A complete inventory of the Omo I lower-limb remains is provided in Table 2.

Pelvic girdle

A large fragment of the left os coxae (KHS 1-60A), together with a small piece of the left iliac crest (KHS 1-60B) attributed to the Omo I individual were discovered during recent fieldwork (Fig. 6). The partial os coxae comprises nearly all of the acetabulum, the ischial tuberosity, and portions of the iliac blade surrounding the greater sciatic notch. Placed in approximate anatomical position, the specimen has a superoinferior dimension of 104.9 mm and a maximum length 148.5 mm, measured along the superior border. The maximum superoinferior diameter of the preserved portion of the iliac blade is 72.5 mm. The acetabulum, missing the superior margin, is large, with a maximum diameter of 55.2 mm (measured superior-anterior to inferior-posterior). Beneath the anterior horn of the lunate surface, the center of the acetabulum retains a number of round, dark-brown mineral encrustations.

The ischial tuberosity is positioned close to the inferior margin of the acetabulum, with a narrow (8 mm) sulcus separating them. Much of the surface of the ischial tuberosity has been worn away, but enough of the cortical shell remains over its superior third to allow its width to be determined as 24.5 mm. The ischial spine, however, has been lost. Cortical bone remains intact posterior to the acetabulum and along the inferior aspect of the greater sciatic notch. The anteroposterior distance from the posteriormost point on the rim of the acetabulum to the greater sciatic notch is 36.8 mm.

The greater sciatic notch is fairly wide, which might be consistent with the identification of Omo I as a female, yet the iliac blade sweeps inferiorly over the posterior end of the notch, which is more consistent with male morphology. Given this inferior projection of the posterior end of the greater sciatic notch, and the large size of the acetabulum, male sex seems more probable than female. However, a very shallow preauricular sulcus, accentuated by two shallow but well-delineated pits, is present between the posterior margin of the greater sciatic notch and the anteroinferior lip of the auricular surface. A preauricular sulcus is more common in female than in male pelves. In a sample of 49 os coxae of individuals of European origin from a nineteenth-century church cemetery in Canada, Rogers and Saunders (1994) reported that 91.6% of individuals could be correctly assigned to sex based on the presence or absence of a preauricular sulcus. Arsuaga and Carretero (1994) found that a well-marked preauricular sulcus was present in 80% of females and absent in 95% of males in a Portuguese (Coimbra) sample consisting of 187 females and 226 males of known sex. The presence of a preauricular sulcus suggests Omo I was most likely female, but the other features of the os coxae do not strongly support this assessment. The assignment of sex from this partial os coxae is presently uncertain.

Table 2
Inventory of Omo I lower-limb specimens

Specimen number		Element	Side	Previous illustration	Notes
Omo 1967 KHS 1-#[a]	MN-#[b]				
5	37	Metatarsal II, base + shaft	Rt	Day et al., 1991 (Fig. 2)	Bone mislabeled "R. m/c II"
14	23	Metatarsal IV, base + proximal shaft	Rt	Day et al., 1991 (Fig. 2)	Bone mislabeled "R m/c III"
21	22	Metatarsal I	Rt	Day et al., 1991 (Fig. 2)	Bone mislabeled "R m/c I"
25	25	Pedal proximal phalanx, ray I	Rt	Day et al., 1991 (Fig. 2)	
26	26	Pedal terminal phalanx, ray I	Rt	Day et al., 1991 (Fig. 2)	
27	28	Cuboid	Rt	Day et al., 1991 (Fig. 2)	Bone mislabeled "R. medial cuneiform"
29A	38	Femur, distal	Rt	Day et al., 1991 (Fig. 2)	Conjoins KHS 1-29B
29B	38-B	Femur, distal diaphysis fragment	Rt	No	New find. Conjoins KHS 1-29A.
35	35	Fibula, distal diaphysis fragment	Rt	Day et al., 1991 (Fig. 2)	
44	24	Metatarsal II or cuneiform II?, base	Lt	No	Identified as "?? Metatarsal base" by Day et al. (1991)
45	29	Navicular	Rt	Day et al., 1991 (Fig. 2)	
46	30	Medial cuneiform	Rt	Day et al., 1991 (Fig. 2)	Bone mislabeled "Cuboid"
47	32	Tibia, diaphysis	Lt	Day et al., 1991 (Fig. 2)	
51A	39	Tibia, distal epiphysis	Rt	Day et al., 1991 (Fig. 2)	Initially composed of 3 fragments glued together, now unglued
51B	None	Tibia, diaphysis	Rt	Day et al., 1991 (Fig. 2)	
52	31	Metatarsal III, base	Rt	Day et al., 1991 (Fig. 2)	Bone mislabeled "MT IV"
59	None	Talus	Rt	No	New find
60A	None	Os coxae fragment	Lt	No	New find
60B	None	Iliac crest fragment	Lt	No	New find

[a] Or revised here.
[b] Assigned by Day et al. (1991).

A large rectangular piece of bone (17.2 mm anteroposterior by 38.0 mm superoinferior) is missing from the external surface of the iliac blade, thereby exposing cancellous bone directly above the apex of the greater sciatic notch. Generally, the internal surface of the os coxae is much better preserved than the bone of the external surface. Still, two prominent step fractures interrupt the internal surface: the posterior fracture courses from the apex of the greater sciatic notch to the superior edge of the fragment, while the anterior fracture runs superiorly across the posterior third of the ischium to the superior edge of the bone. The latter fracture has displaced the edges of the preserved bone by 7.2 mm at the arcuate line. The internal surface of the ischium also bears a large number of very small cracks reminiscent of surface damage from sun weathering prior to burial and fossilization. The auricular surface, which measures 58.2 mm in length, is well preserved. Some of its surface has a very fine-grained, granular texture, and it also bears a series of very small ripples suggestive of young adult morphology (i.e., 20–30 years of age). This age estimate agrees with that proposed by Day (1969) based on the state of cranial-suture closure. He observed that Omo I's sagittal suture is closed and obliterated internally while the coronal and lambdoidal sutures are open, which suggests that the specimen was a young adult and probably younger than Omo II.

Fig. 6. Newly recovered pelvic fragments: (a) left os coxae (KHS 1-60A), lateral view; (b) fragment of the left iliac crest (KHS 1-60B), lateral view. Scale bar = 4 cm.

At the point where the apex of the auricular surface meets the arcuate line, the surface has a mediolateral diameter of 17.3 mm. The ilium extends 21.9 mm posterior to the apex of the auricular surface. The second, smaller os coxae fragment represents the iliac tubercle along the left iliac crest; it measures 52.5 mm anteroposteriorly by 32.9 mm superoinferiorly. The margin of the tubercle bears a series of anterolaterally projecting osteophytes reflecting the origin of the tensor fascia latae. The maximum mediolateral thickness of the iliac tubercle is 19.8 mm.

Thigh

The specimen KHS 1-29 is the distal end of a right femur. In the course of recent fieldwork, a second fragment of the right femoral shaft was discovered; this new specimen (KHS 1-29B) conjoins perfectly with the original specimen (now referred to as KHS 1-29A) along an irregular break through the posterior face of cortical bone (Fig. 7). Specimen KHS 1-29A preserves the femoral condyles, patellar surface, popliteal fossa, and a ~32-mm-long segment of metaphysis broken roughly along the horizontal plane approximately 67 mm above the inferior intercondylar articular surface. The lateral condyle is well preserved, as is the lateral epicondyle, whereas the medial condyle has lost its medial half together with the medial epicondyle and an adjacent surface of bone from the medial aspect of the femoral metaphysis. The superior extent of the patellar articular surface has also been heavily abraded. The posterior aspect of the intercondylar notch and the popliteal surface

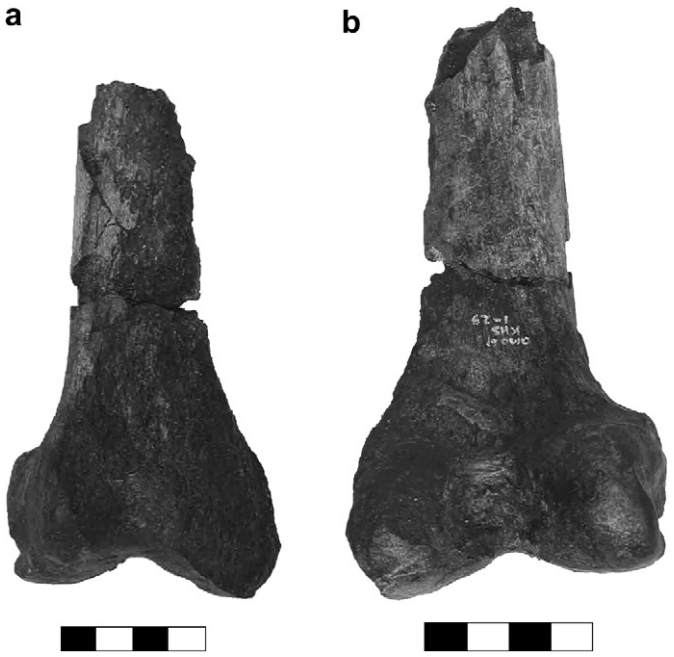

Fig. 7. Distal end of the right femur (KHS 1-29A) and the newly recovered conjoining piece of the distal femoral diaphysis (KHS 1-29B): (a) anterior view; (b) posterior view. Scale bars = 4 cm.

are preserved intact. The superomedial border of the patellar articular surface has a minor amount of periarticular osteophyte development, as does the medial margin of the posterior aspect of the lateral condyle, while the remaining periarticular surfaces of the condyles are relatively free of osteophytes. The popliteal surface above the lateral and medial condyles displays small bony elevations around the areas for the origins of the lateral and medial bellies of gastrocnemius. The deeply excavated intercondylar surface presents small osteophytic growths around the insertion site for the medial border of the anterior cruciate ligament. The lip of the lateral supracondylar line becomes crisply defined immediately above the popliteal surface, although it maintains a low relief, projecting only about 1 mm above the shaft. The lip of the medial supracondylar line is also discernible along the back of the femoral diaphysis, but it is much less clearly defined than the lateral lip.

The new specimen (KHS 1-29B) is well preserved along its posterior and lateral aspects, but its anterior half is crushed, resulting in the loss of large pieces of cortical bone. The medullary cavity is filled with a hard, dark-brown matrix. The new fragment is some 66 mm in length; when conjoined with the distal fragment (KHS 1-29A), the total length of preserved right distal femur is ca. 130 mm from the inferior intercondylar articular surface; maximum superoinferior length is 138.7 mm. The overall impression from the refitted distal femur is of a long, slender shaft arising from a relatively small distal epiphysis. A series of measurements for the distal femur are provided in Table 3. Day et al. (1991) observed grooves left on the condyles by the lateral and medial menisci, and they stated that the grooves separate the condylar surface for the patella from the surface for the menisci. The grooves are faintly developed. Day et al. (1991) also noted the presence of a very marked groove for the lateral collateral ligament on the lateral aspect of the lateral condyle. This groove is certainly large and visible just inferior to the lateral epicondyle. The tendon of the popliteus muscle originates inferior to the insertion of the lateral collateral ligament. A slight ridge separates the attachment areas for the ligament and tendon of the muscle on the Kibish specimen.

Table 3
Measurements of the right distal femur of Omo I (specimen KHS 1-29A conjoined with KHS 1-29B)

Description of measurements	Measurements (mm)
Bi-epicondylar breadth	(76.3)
Anterior patellar notch width	(30.5)
Maximum breadth, inferior condylar surface	(70.9)
Anteroposterior shaft diameter (just below proximal break)	((29.0))
Mediolateral shaft diameter (just below proximal break)	(31.1)
Mediolateral shaft diameter (1 cm above joint between main fragments)	(33.9)
Maximum width, superior extension of medial condyle (posterior view)	(22.0)
Maximum width, superior extension of lateral condyle (posterior View)	25.4

Measurements in parentheses are minimum dimensions for life due to heavy abrasion of portions of the specimens.

Leg

Portions of both the right and left tibiae from the Omo I individual have been recovered. An unnumbered fragment preserves a portion of the right tibial diaphysis. This specimen is assembled from four smaller pieces and has an overall length of 118 mm. The posterior aspect of the shaft is intact, as is the central portion of the lateral side, but the anterior and medial borders of the shaft are missing. There is no sign of the nutrient foramen proximally. Day et al. (1991) noted the presence of a groove for the nutrient foramen on the internal surface of the proximal portion of the fragment. However, the cortical bone is thick anteriorly and posteriorly, suggesting that the specimen most likely represents the tibial midshaft and diaphysis immediately distal to midshaft. The interosseous line is undetectable. Damage precludes accurate measurements of the anteroposterior and mediolateral dimensions of the shaft. Nevertheless, the shaft measures close to 32 mm anteroposteriorly by 22 mm mediolaterally at the level of the proximal break. These dimensions are similar to those recorded for the left tibial diaphysis (see below) and indicate very platycnemic tibiae. The cortical wall measures approximately 10 mm in anterior thickness, 9 mm posteriorly, and 6 mm laterally at the level of the proximal break.

Specimen KHS 1-51 is the distal epiphysis of the right tibia. Day et al. (1991: 604) incorrectly described this specimen as a left tibia but correctly listed their specimen MN 39 (=KHS 1-51) as representing a distal right tibia in later detailed descriptions and in Table 1 of the same publication. At the time of study by the present authors, the specimen consisted of three major fragments glued together. It was determined by one of us (FEG) that the superiormost fragment, and possibly the middle fragment, did not fit with the distal end of the tibia. It is now unclear whether the two smaller distal shaft fragments were glued to the distal epiphysis when illustrated in Fig. 2 of Day et al. (1991). Thus, in the description that follows, we restrict specimen KHS 1-51A to refer specifically to the distal epiphysis of the right tibia, while KHS 1-52B designates the remainder of the right tibial diaphysis.

The distal epiphyseal fragment measures 61.1 mm superoinferiorly by 44.2 mm mediolaterally. The cortical bone on the posterior side of the fragment is preserved, but its surface is slightly eroded. The posterior border of the contact surface for the fibula has suffered more damage, resulting in completely abraded cortical bone and exposed cancellous bone. The surface of the anterior face of the epiphysis is also severely abraded, exposing matrix that fills the medullary cavity except for the lateralmost 10.3 mm of the bone along the fibular facet. Approximately the anteriormost third of the medial malleolus is also missing. In inferior view, the epiphysis appears to have an unusual triangular shape with a compressed

medial margin. The talar facet is triangular in outline, measuring a maximum of 37.0 mm anteroposteriorly and a maximum of 41.0 mm mediolaterally. In contrast, most human distal tibial epiphyses appear rectangular in shape. The apparently unusual appearance of the Omo I distal tibia may be a product of the abrasion that has affected the anteromedial side of the fragment. The largely intact talar articular surface shows little sign of abrasion. However, the anterior border of the talar articular surface is cracked and missing, notably along the medial side. The remaining articular surface articulates very well with the newly recovered right talus from the KHS site. The maximum anteroposterior diameter of the lateral side of the distal end of the tibia measures 37.6 mm, while the anteroposterior diameter of the medial side (measured at the lateral edge of the medial malleolus) is 25.0 mm, and the maximum mediolateral diameter of the distal epiphysis measures 57.3 mm. A large sulcus is present on the lateral edge of the distal tibia at the origin site of the anterior inferior talofibular ligament. Due to surface abrasion, it is impossible to say whether the specimen bore a squatting facet. Day et al. (1991: 605) noted the presence of a very marked groove on the posterior face of the medial malleolus for the tibialis posterior's tendon and its synovial sheath. We observed a slight groove on the posterior face of the medial malleolus, but do not agree that it is "very marked." Abrasion of the surrounding area may account for some but not all of this difference in our observations.

The shaft of the left tibia, KHS 1-47, has been assembled from a number of smaller fragments, with a maximum length of 134 mm (Fig. 8). The distal end of the specimen likely approximates the midshaft level; at this point, the diaphysis measures 23.5 mm mediolaterally by 35.5 mm anteroposteriorly. This results in a very platycnemic tibial shaft. The anterior tibial crest is blunt. The interosseous crest is very weakly developed and expressed only as a slight change in the curvature of the medial surface. Much of the medial surface, however, is cracked and damaged. The cortical wall measures 18.4 mm thick anteriorly, 5.5 mm thick medially, 5.3 mm thick laterally, and 7.9 mm thick posteriorly at the level of the distal break.

A 95.5-mm-long shaft fragment of the distal right fibula of Omo I is preserved (KHS 1-35). The specimen is broken just proximal to the lateral malleolus. The proximal shaft bears a small crest bordering a slight depression for the origin of the peroneus brevis muscle. The crest extends 33 mm down the shaft, gradually becoming less pronounced in relief. The proximal end of the shaft measures 13.3 mm anteroposteriorly by 10.0 mm mediolaterally.

Fig. 8. Diaphysis of the left tibia (KHS 1-47): (a) lateral view, (b) medial view. Scale bar = 4 cm.

The distal quarter of the shaft bulges outwardly and has thinner cortical bone, features that probably document the presence of an old, heavily remodeled callus from the repair of a fracture to this part of the fibular diaphysis. The shaft becomes considerably wider at the level of the callus, measuring 19.1 mm anteroposteriorly by 15.2 mm mediolaterally near the superior extent of the callus. Below this point, the posterior portion of the shaft is broken away, and no additional measurements are possible.

Ankle and foot

Much of the right foot of the Omo I individual is known (Fig. 9), including a recently discovered well-preserved, complete right talus (KHS 1-59). The talus has a fairly small trochlear surface, a disproportionately large head, and a laterally projecting facet for the lateral malleolus. Neandertal and some recent human tali, notably those of Khoe-San individuals, also tend to have very laterally flaring facets for the lateral malleolus (Kaufmann, 1941; Rhoads and Trinkaus, 1977; Gambier, 1982; Trinkaus, 1983). A deep dorsal fossa with a crestlike osteophytic lip lies between the talar and navicular facets and may represent a squatting facet (Boulle, 2001). There is an arthritic extension of the medial edge of the trochlea. The posterior aspect of the talus has suffered some abrasion, obscuring the impression for the tendon of flexor hallucis longus. Any measurement taken from this posterior point should therefore be considered a minimum for the dimension in life. Dimensions of the talus are reported in Table 4.

Figure 9i depicts the well-preserved right navicular (KHS 1-45). The navicular is 35 mm wide (mediolaterally), 23.5 mm high (dorsoplantarly), and 17.5 mm long (anteroposteriorly); additional measurements are listed in Table 5. In absolute terms, the dimensions of the Omo I navicular fit comfortably within the range expressed by the Qafzeh and Skhul fossils, except for the thickness of the medial cuneiform facet, which is smaller in Omo I (14.0 mm) compared to the Levantine sample (16.5–18.5 mm) (Vandermeersch, 1981). The Omo I navicular preserves a large, concave talar facet and three convex distal facets for articulation with the cuneiforms. As noted by Day et al. (1991), the articular facet for the medial cuneiform is roughly quadrangular, while the facets for the intermediate and lateral cuneiforms are more triangular in outline. The medial border of the lateral facet is notably depressed relative to the intermediate facet. While this condition is found infrequently in modern human homologues, according to Day et al. (1991), it is within the range of modern morphological variation. Our observations confirm the presence of a deep groove for the tendon for tibialis posterior along the plantar aspect of the large prismatic medial tuberosity, as well as the presence of a prominent plantar point, as highlighted by Day et al. (1991). The well-developed plantar point suggests a similarly developed plantar calcaneonavicular or spring ligament in the Omo I individual.

Specimen KHS 1-27 is a complete right cuboid (Fig. 9h). The element has suffered surface abrasion, resulting in exposed trabecular bone on the lateral side just superior to the start of the peroneal groove. There is also some abrasion of the plantar surface, especially proximally, but this does not obscure the peroneal groove. The specimen has a maximum anteroposterior dimension of ca. 28 mm and a maximum mediolateral dimension of ca. 23.9 mm; however, these orientations are only approximate, and abrasion has affected the mediolateral dimension. The cuboid has a large articular surface for the calcaneus that measures 25 mm wide by 15 mm high, with the superior and lateral portions missing. Separate distal facets for metatarsal IV and metatarsal V are preserved with only slight damage to the superior rim. These two distal facets are separated by a beaklike process arising from a dorsoplantar crest. The maximum dorsoplantar height of the cuboid is 21.2 mm. The medial facet for the lateral cuneiform is

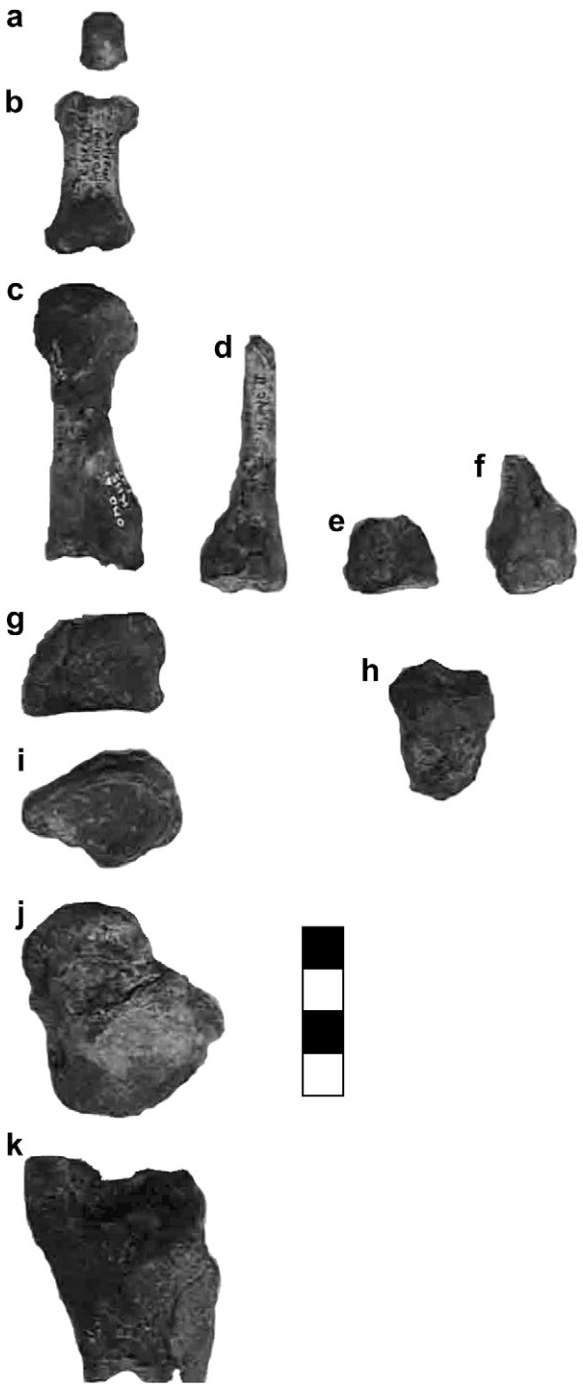

Fig. 9. Right foot: (a) terminal phalanx of ray I (KHS 1-26), dorsal view; (b) proximal phalanx of ray I (KHS 1-25), dorsal view; (c) metatarsal I (KHS 1-21), lateral view; (d) metatarsal II fragment (KHS 1-5) medial view; (e) base of metatarsal III (KHS 1-52), dorsal view; (f) base of metatarsal IV (KHS 1-14), medial view; (g) medial cuneiform (KHS 1-46), dorsal view; (h) cuboid (KHS 1-27), dorsal view; (i) navicular (KHS 1-45), posterior view; (j) talus (KHS 1-59), superior view; (k) distal tibia (KHS 1-51), anterior view. Scale bar = 4 cm.

intact and measures 15.5 mm anteroposteriorly by 12.0 mm dorsoplantarly. Day et al. (1991) noted the presence of a prominent tubercle for the attachment of the calcaneocuboid ligament.

The complete right medial (first) cuneiform (KHS 1-46) (Fig. 9g) has suffered surface abrasion, especially on the distal portion of the medial surface. The lateral edge of the proximal articular surface is also mildly abraded. The bottom half of the element has been glued onto the top half, with a faint line marking the junction. The first

Table 4
Measurements of the right talus of Omo I (specimen KHS 1-59) (following Martin and Saller, 1957)

Description of measurements	Measurements (mm)
Length of talus (M1)	(53.8)
Width of talus (M2)	43.1
Height of talus (M3)	27.5
Length of trochlea (M4)	26.2
Width of trochlea (M5)	(25.3)
Posterior width of trochlea ($M5_1$)	((21.3))
Length of head and neck (M8)	20.3
Length of head (M9)	(30.1)
Width of head (M10)	(19.8)
Length of posterior calcaneal articular surface (M12)	(34)
Width of posterior calcaneal articular surface (M13)	20.3
Length of head and neck (T12)[a]	21.0
Physiological height (T13)[a]	23.2
Lateral malleolar facet breadth (T14)[a]	10.7
Articular breadth (T15)[a]	26.9

Measurements in parentheses are minimum dimensions for life due to heavy abrasion of portions of the specimen.
[a] Additional talar dimensions from Pearson (1997).

cuneiform preserves a rounded facet for the navicular and a flat, kidney-shaped facet for metatarsal I. The superior aspect of the lateral surface has a long facet for the intermediate cuneiform, as well as a small facet immediately distal to it for metatarsal II. The medial cuneiform articulates well with the base of the first metatarsal and also demonstrates that roughly 4–5 mm of bone is missing from the plantar surface of the base of the first metatarsal, thus decreasing its apparent dorsoplantar height. Additional measurements of the medial cuneiform can be found in Table 6.

Specimen KHS 1-21 is a right metatarsal I (MT 1; Fig. 9c). The element is complete save for a piece of shaft missing in the middle of the inferior aspect. There is some abrasion of the plantar part of the base, resulting in a 4–5-mm loss of bone. The metatarsal has been broken at midshaft and has been glued back together. A chip of bone is missing from the midshaft of the lateral side and a larger (13.2 mm anteroposterior by 10 mm mediolateral) chip is missing anterior to the midshaft break on the plantar surface. Additional damage has accrued along the medial edge of the distal articular surface and to the median ridge of the plantar aspect of the distal articular surface, as well as some abrasion to the lateral side of the nonarticular bone of the distal epiphysis. Some arthritic lipping is present on the medial side immediately proximal to the anterior articular surface of the head.

As previously noted (Day et al., 1991), the base bears a moderately concave, kidney-shaped articular facet for the medial cuneiform and extends into a well-developed tubercle.

Measuring 64.8 mm long, the first metatarsal of Omo I falls just beyond the range of MT 1 length (50.0–64.5 mm) observed in the Qafzeh/Skhul sample (McCown and Keith, 1939; Vandermeersch, 1981). Additional measurements of the MT 1 are listed in Table 7. In all dimensions except articular length, the Omo I first metatarsal

Table 5
Measurements of the right navicular of Omo I (specimen KHS 1-45) (following Martin and Saller, 1957)

Description of measurements	Measurements (mm)
Navicular width (M1)	37.8
Navicular height (M2)	28.1/25.7[a]
Length of the posterior facet (M3)	28.5
Width of the posterior facet (M4)	21.5
Width of the cuneiform facet (M6)	36.7
Thickness of the facet for cuneiform III (M7)	9.0
Thickness of the facet for cuneiform III (M8)	14.0

[a] The smaller measurement does not include the dorsally projecting point of the facet separating the cuneiform facets.

Table 6
Measurements of the right medial cuneiform of Omo I (specimen KHS 1-46) (following Martin and Saller, 1957)

Description of measurements	Measurements (mm)
Length of the plantar side (M1)	23.7
Length of the dorsal side (M2)	22.3[a]
Height of the proximal (navicular) articular surface (M3)	19.9
Height of the distal (metatarsal) articular surface (M4)	31.1
Maximum mediolateral diameter of the proximal articular surface	17.8
Maximum dorsoplantar diameter of proximal articular surface	35.1

[a] Measurement taken approximately 1 cm deep to the dorsal surface.

fits comfortably within the range of the Qafzeh and Skhul individuals and is notably similar to Qafzeh 8 (Vandermeersch, 1981). Byers et al. (1989) developed methods to estimate stature from the length of the first metatarsal. Their formulae give the following stature estimates for Omo I: 169.7 ± 5.1 cm (among African-American males), 162.4 ± 5.1 cm (among African-American females), and 172.3 ± 6.5 cm (among pooled African-Americans and European-Americans of both sexes). These estimates of stature for Omo I are much lower than the stature estimated from humeral length. It is possible that the formulae developed by Byers and colleagues do not work as well for individuals with very linear bodies such as Omo I or the early modern skeletons from Skhul and Qafzeh.

Specimen KHS 1-5 is a fragment of the right metatarsal II (Fig. 9d). The specimen measures 60.8 mm in length, preserving the base and nearly the entire shaft, which is broken just proximal to the expansion for the head. Also preserved are both lateral facets for the lateral cuneiform and metatarsal III, and the medial facet for the medial cuneiform. The diaphysis of the second metatarsal appears quite slender. Its dorsal surface bears a slight longitudinal keel, but no distinct lines for the attachment of dorsal interosseous muscles. The shaft dimensions, measured 40 mm from the proximal end, are 8.8 mm dorsoplantarly and 7.5 mm mediolaterally. The medial facet for the articulation with the first metatarsal is clearly defined and bordered by a slight arthritic lip; the facet is small, measuring 4.4 mm proximodistally by 7.0 mm superoinferiorly. The superior articular facet for metatarsal III is also clearly visible and bordered by arthritic lipping. The inferior articular facet for metatarsal II is only partially preserved: its plantar half has been destroyed by abrasion, exposing the underlying trabecular bone. The maximum mediolateral diameter of the dorsal surface of the base measures 15.3 mm, while the maximum dorsoplantar diameter of the base is 21.1 mm.

Specimen KHS 1-52 is the base of a right metatarsal III (Fig. 9e). The maximum length of the fragment is 17.3 mm. The surface of the bone is slightly eroded, but most morphological features are visible.

Table 7
Measurements of the right metatarsal I of Omo I (specimen KHS 1-21) (following Martin and Saller, 1957)

Description of measurements	Measurements (mm)
Articular length (M1)	64.8
Midshaft breadth (M3)	14.9
Midshaft height (M4)	14.6
Proximal maximum breadth (M6)	20.6
Proximal maximum height (M7)	((25.7))[a]
Distal maximum breadth (M8)	n/a
Distal maximum height (M9)	20.5

[a] Proximal maximum height as preserved, with damage to the inferior aspect of the base. We estimate the actual proximal maximum height to be between 29.7 mm and 30.7 mm.

The plantarmost aspect of the proximal articular surface is eroded, exposing cancellous bone. The specimen preserves the facet for the lateral cuneiform and, laterally, for metatarsal IV, which is rimmed by a very small ring of osteophytic bone. On the medial side, the articular facet for metatarsal II has been destroyed by surface abrasion. As far as can be judged from the preserved portions, the proximal articular surface of the base is unaffected by arthritic changes. The base measures a maximum of 14.5 mm mediolaterally across its dorsal surface and has a maximum dorsovolar height of 22.5 mm.

Figure 9f depicts specimen KHS 1-14, the base and proximal portion of the shaft of the right metatarsal IV. The fragment preserves 33.9 mm in maximum length. As observed by Twist (1985/1986), the proximal end bears a concave lateral facet for metatarsal V that is confluent with the articular facet for the cuboid. On the medial side, most of the facet for metatarsal III has been lost. The bottom of the base displays moderate osteophytic development, and an osteophytic lip also runs along the dorsal margin of the medial side. The maximum mediolateral breadth of the proximal end measures approximately 11.5 mm, although abrasion to the superomedial part of the articular surface makes this a minimum estimate. The dorsal surface of the base has a maximum width of 10.8 mm and a maximum dorsalplantar height of approximately 14.0 mm (a minimum due to erosion of the plantar surface).

The specimen bears an interesting series of pathological changes. A 16-mm-long roughened outgrowth can be seen on the dorsal surface, starting 3.5 mm distal to the proximal end. This osteophytic mass extends onto the medial side of the base and the proximal shaft, obscuring the facet for the third metatarsal, and forming a mound of osteophytic growths measuring 16.6 mm superoinferiorly by 16.0 mm proximodistally. A second notable pathological change is a large exostosis extending from the base onto the plantar surface of the shaft. This outgrowth measures 16.9 mm proximodistally by 7.3 mm mediolaterally. The inferior surface of the exostosis is flat. The final pathological change in this element is a minor amount of arthritic lipping around the contact facet for the fifth metatarsal.

Specimen KHS 1-44 was tentatively described by Day et al. (1991) as the base of an indeterminate metatarsal. The attribution of this fragment remains uncertain: it may be the base of a left metatarsal II, or alternatively, it could be an intermediate cuneiform. The fragment is small, retaining approximately two-thirds of its proximal articular surface. It is badly crushed on the lateral side and eroded on its medial side and on the plantar surface of the base. The medial and lateral damage is severe enough to obscure the articular surfaces. The dorsal surface measures 15.9 mm mediolaterally at its widest point, which is located just distal to the proximal articular surface. The maximum proximodistal length of the fragment is 21.5 mm.

The specimen KHS 1-25 is a complete right proximal pedal phalanx of ray I (Fig. 9b). It has a maximum length of 37.4 mm. Some small osteophytes are present along the medial and lateral aspects of the plantar margin of the proximal articular surface; these project no more than 2–3 mm and do not impinge upon the articular surface itself. The distal epiphysis bears more substantial development of osteophytes on and around the articular surface. The maximum width of the distal articular surface is 20.0 mm.

Specimen KHS 1-26 is a right terminal pedal phalanx of ray I (Fig. 9a). The element, with a preserved length of 14.5 mm, lacks the base and apical tuft. It is still apparent, however, that the base of the shaft is asymmetrical, with a longer lateral than medial part, which would make the axis of the great toe point slightly laterally. The base of the fragment preserves approximately half of the insertion pit for the tendon of flexor hallucis longus. The distal end of the plantar surface features the beginnings of tiny bony struts of support for the apical tuft. The maximum width of the proximal

end is 11.9 mm, and the maximum dorsoplantar height of the proximal end is 6.6 mm.

Estimation of body mass

Estimated body mass provides a final detail that may be gleaned from the remains of the upper and lower limbs of Omo I. Neither of the femoral heads is preserved, but the skeleton preserves two dimensions that are closely correlated with the vertical diameter of the femoral head: the maximum proximodistal diameter of the left humeral head and the maximum diameter of the left acetabulum measured from superoventral to posterodorsal (Pearson, 1997). In order to estimate femoral head size—one of the best dimensions for estimating body mass—a large worldwide sample of recent humans of both sexes (Pearson, 1997, 2000b) in which data were available for the vertical femoral head diameter (FHD), maxiumum acetabular diameter (ACD), and proximodistal (vertical) diameter of the humeral head (HHD) was used to create a multiple regression equation to estimate Omo I's FHD. For the equation, a recent human sample consisting of 368 individuals was used. The least-squares regression indicated that most of the variance in FHD could be predicted from the two variables ($r^2 = 0.899$; $p < 0.0001$; standard error of the estimate = 1.24 mm) and produced the following prediction equation:

$$\mathrm{FHD} = -0.421 + 0.316(\mathrm{HHD}) + 0.598(\mathrm{ACD}).$$

Omo I's left HHD measures 46.5 mm proximodistally and the maximum diameter of its acetabulum is 55.2 mm, which produces an estimate of 47.28 ± 1.24 mm for its FHD.

Applying the formula to estimate body mass from FHD published by Grine et al. (1995) to the estimate of FHD from acetabular diameter produces an estimate of 70.73 ± 4.3 kg (plus or minus an additional 2.81 kg from the uncertainty surrounding the estimate of femoral head diameter).

Compound errors from a series of estimates (two in this case) are a common problem in paleoanthropology (Smith, 1996). In the present case, one would wish to know the overall uncertainty introduced by the two estimates. The error introduced by each estimate is independent of and orthogonal to the other estimate. Given this fact, the overall error is analogous to the hypotenuse of a right triangle in which each of the other two sides is the standard error of each estimate. Using the Pythagorean theorem, this simple method indicates the overall estimate should be 70.73 ± 5.14 kg.

Morphological description: axial postcranial skeleton

Numerous fragments of ribs, costal elements, and vertebrae have been recovered; however, there are no preserved portions of the sacrum or the coccyx of the Omo I individual. A complete inventory of postcranial axial remains attributed to Omo I is listed in Table 8.

Ribs

There are six fragments that have been attributed to proximal right ribs: one fragment preserves the head and vertebral facet, three preserve only the head, and two preserve only the vertebral facet. In addition, there are five proximal fragments from left ribs. Three of these preserve the head and vertebral facet, one preserves only the head, and one preserves only the vertebral facet. All rib fragments have been sided by the position of the vertebral articular facet, which is known to be on the inferior surface of the rib, and by observing that the superior demifacet of the head is larger than the inferior demifacet. Thirty-seven costal shaft fragments, which cannot be sided, have also been recovered. Of the costal elements, 36 fragments were excavated in the 1967 field season, and one was discovered during recent fieldwork.

Table 8
Inventory of Omo I axial postcranial specimens

Specimen number[a]		Element
None	KHS 1-53	Proximal rib fragments (6 Rt, 5 Lt)
None	KHS 1-54	Costal shaft fragments (36 found in 1967; 1 found recently)
V1	KHS 1-55	Axis (C2), spinous process
V2	KHS 1-55	Cervical vertebra, spinous process
V3	KHS 1-55	Cervical vertebra, body
V4	KHS 1-55	Cervical vertebra
V5	KHS 1-55	Cervical vertebra
V6	KHS 1-55	Cervical vertebra (lower), spinous process
V7	KHS 1-55	Thoracic vertebra, lamina
V8	KHS 1-55	Thoracic vertebra, Rt lamina + spinous process fragment
V9	KHS 1-55	Thoracic vertebra, spinous process
V10	KHS 1-55	Thoracic vertebra, spinous process
V11	KHS 1-55	Thoracic vertebra, transverse process
V12	KHS 1-55	Thoracic vertebra, Lt lamina + transverse process
V13	KHS 1-55	Thoracic vertebra, transverse process
V14	KHS 1-55	Thoracic vertebra, transverse process
V15	KHS 1-55	Thoracic vertebra (lower), transverse process + Rt lamina frag.
V16	KHS 1-55	Lumbar vertebra, spinous process + Rt lamina
V17	KHS 1-55	Lumbar vertebra, Rt inferior zygopophysis

[a] The specimen numbers for costal and vertebral specimens were assigned by John Fleagle and colleagues.

Vertebrae

Since there have been no previously assigned museum or molding numbers for the Kibish vertebral fragments, the Omo I vertebral specimens have been assigned reference numbers by the present authors. The recovered vertebral elements include six cervical fragments, nine thoracic fragments, and two lumbar fragments; all vertebral specimens are depicted in Fig. 10.

Specimen V1 is the spinous process of the axis (C2), preserving a short segment of the laminae. The spine is 17 mm long from the roof of the vertebral canal to its apex. Superiorly, the spine has a single crest (4 mm wide) that divides inferiorly. The right side of the spine has been destroyed. The spine measures 15 mm deep superoinferiorly.

Specimen V2 is an incomplete spinous process of an indeterminate cervical vertebra. It preserves short segments of the laminae. The spine is broken before its terminal split; the preserved spine is 15 mm long from the roof of the vertebral canal.

Specimen V3 is the body of an indeterminate cervical vertebra, preserving a small fragment of the right pedicle. The anteroinferior margin of the body has suffered damage. The superior concave surface is 20.5 mm wide from lip to lip; the inferior surface is 20 mm wide. The body is 16 mm deep anteriorly.

Specimen V4 is a partial indeterminate cervical vertebra, consisting of the body, the right and left pedicles, the costal element, anterior and posterior tubercles, superior and inferior zygopophyses, and part of the lamina. The foramen transversarium of V4 is 4.7 mm wide. The superior and inferior zygopophyses are separated by a 9.5-mm-thick lamina. The vertebral canal is a maximum of 22 mm wide. The body is 16 mm deep; the superior concave surface measures 21 mm from lip to lip, and the inferior surface is 19.5 mm wide.

Specimen V5 is another partial indeterminate cervical vertebra. This specimen preserves the body, the right pedicle, and part of the right lamina with superior and inferior zygopophyses. The body is 15 mm deep, the superior concave surface is 21 mm wide (lip to

Fig. 10. Vertebral fragments: (a) spinous process of the axis (KHS 1-55-V1); (b) cervical spinous process (KHS 1-55-V2); (c) body of a cervical vertebra (KHS 1-55-V3); (d) fragmentary cervical vertebra (KHS 1-55-V4); (e) fragmentary cervical vertebra (KHS 1-55-V5); (f) spinous process and laminae of a lower cervical vertebra (KHS 1-55-V6); (g) lamina of a thoracic vertebra (KHS 1-55-V7); (h) spinous process and right lamina of a thoracic vertebra (KHS 1-55-V8); (i) spine of a thoracic vertebra (KHS 1-55-V9); (j) partial spine of a thoracic vertebra (KHS 1-55-V10); (k) transverse process of a thoracic vertebra (KHS 1-55-V11); (l) left lamina and transverse process of a thoracic vertebra (KHS 1-55-V12); (m) transverse process of a thoracic vertebra (KHS 1-55-V13); (n) transverse process of a thoracic vertebra (KHS 1-55-V14); (o) spinous process of a lumbar vertebra (KHS 1-55-V16); (p) transverse process of a thoracic vertebra (KHS 1-55-V15); (q) right zygopophysis of a lumbar vertebra (KHS 1-55-V17). Scale bar = 10 cm.

lip), and the inferior surface is 20 mm wide. The superior and inferior zygopophyses are separated by a 10-mm-thick lamina. This element seems to articulate well with specimen V4, suggesting that it followed specimen V4 caudally in the vertebral column of Omo I.

The final cervical fragment is specimen V6, which is the spinous process of a lower cervical vertebra with very short segments of both laminae. The spine is 25 mm long from the roof of the vertebral canal. The spinous tip broadens to 10 mm from a waist of 6 mm, but is only incipiently bifid. The spine measures 9 mm superoinferiorly.

Nine isolated thoracic vertebral elements have been recovered, comprising mostly spines and transverse processes. None of these thoracic elements articulate with one another. Specimen V7 is the lamina of an indeterminate thoracic vertebra. It preserves the left inferior zygopophysis, which is 8 mm broad. The complete fragment measures 24 mm wide by 21 mm superoinferiorly.

Specimen V8 is part of a spinous process and right lamina of an indeterminate thoracic vertebra. The tip of the spine is broken away, but 27 mm (measured from the roof of the vertebral canal) of the spine remains. The spine is 4 mm thick and 14 mm deep superoinferiorly. The right lamina is broken just inferior to the superior zygopophysis. The element has a very long inferior zygopophysis (12 mm).

Specimen V9 is the spine of another indeterminate thoracic vertebra. This spine is nearly complete and includes a small portion of the left lamina. The spine is 30 mm long from the roof of the vertebral canal, and superoinferiorly 11 mm deep. The tip of the spine broadens to 6 mm from a waist of 4.5 mm.

Specimen V10 is part of the spine of an indeterminate thoracic vertebra preserving the roof of the vertebral canal, but missing the tip. The piece is 20 mm long as preserved. The inferior margin is intact, while the superior margin is damaged. The spine is 3.0 mm broad mediolaterally.

Specimen V11 is the transverse process of a thoracic vertebra; the side from which it derives is uncertain. The V11 process is 21 mm long, with a costal facet measuring ca. 9.0 mm broad.

Specimen V12 is the left lamina and transverse process of a thoracic vertebra. The lamina is preserved to the base of the spine, and it preserves the inferior zygopophysis. The superior zygopophysis is present, but its articular surface is eroded. The transverse process is ca. 17 mm long, and the costal facet is ca. 7 mm in diameter.

Specimen V13 is the transverse process of an indeterminate thoracic vertebra, comprising a pedicle and the margin of the lamina on the left side. The transverse process is complete, measuring 17 mm in length with a ~9.0-mm-wide costal facet.

Specimen V14 is the transverse process of a thoracic vertebra. The specimen preserves part of the right lamina. The anterior margin of the tip of the transverse process is damaged but otherwise complete. It is ca. 19 mm long and has a deeply concave, 11-mm-wide costal facet. The lamina preserves a large part of the superior zygopophysis and a complete, 13-mm-long inferior zygopophysis.

Specimen V15 is the transverse process of a lower thoracic vertebra preserving part of the right lamina. The transverse process is short and stocky, measuring about 17 mm long, 12 mm superoinferiorly, and 11 mm thick. A poorly preserved costal facet is evident. The lamina is broken just below the superior zygopophysis. The inferior zygopophyseal facet is approximately 10 mm broad.

Only two fragments of lumbar vertebrae have been recovered from the KHS site. Specimen V16 is the spinous process of an indeterminate lumbar vertebra that preserves the right lamina. The apex of the spine is broken off; the remaining portion of the spine measures 17 mm deep superoinferiorly by 6 mm wide. The right lamina, which is broken off at the root of the pedicle, preserves part of the inferior zygopophysis.

The second lumbar specimen, V17, is the right zygopophysis of an indeterminate lumbar vertebra. The fragment is approximately 30 mm long, preserving a ~4-mm-by-12-mm, gently concave articular facet. The zygopophysis is broken at the root of the pedicle.

Conclusions

The descriptions of the Omo I skeleton provided here confirm the specimen's status as the earliest known example of an anatomically modern human (Day, 1969, 1972; Day et al., 1991). Fieldwork designed to clarify the stratigraphy and determine absolute age of the Omo Kibish fossils succeeded in identifying the original spot from which Omo I was recovered and further excavations at the site yielded seven additional fragments of the skeleton. The new specimens include a middle and a distal manual phalanx; a right talus; two fragments of the left os coxae including a large fragment of the left os coxae that includes the acetabulum, auricular surface, and greater sciatic notch, and a small fragment

that preserves the iliac tubercle; a portion of the distal diaphysis of the right femur that conjoins to the original distal epiphysis of the right femur; and a costal fragment.

The brief analyses of aspects of Omo I's morphology highlight some of the unusual features in the skeleton including: medially facing radial tuberosities in both the right and especially left radii, a laterally flaring facet on the talus for the lateral malleolus, and reduced dorsovolar curvature of the base of metacarpal I. These features are shared with Neandertals, some early modern humans from Skhul and Qafzeh, as well as some individuals from the European Gravettian. While it once may have been reasonable to interpret the presence of these "Neandertal-like" features in Eurasian early modern humans as potential evidence of gene flow from neighboring and contemporaneous Neandertal populations, the presence of these features in Omo I raises the distinct possibility that Eurasian early modern humans inherited these features from an African ancestor rather than Neandertals. Other aspects of Omo I, particularly the large projection of its coronoid process of the right ulna relative to its olecranon process align the specimen with recent humans, in contrast to specimens such as the Klasies River Mouth and Border Cave ulnae, which have a relatively underdeveloped coronoid process (Churchill et al., 1996; Pearson and Grine, 1996) in common with the Baringo ulna (Solan and Day, 1992), KNM-WT 15000 (Walker and Leakey, 1993), and australopiths (Drapeau, 2004). Additional studies of the morphological affinities and phylogenetic implications of the Omo I remains are underway.

The new analyses of the Omo I skeleton also reveal some basic information about the individual's sex, age, stature, body mass, and physique. Unfortunately, the fragments of the os coxae do not unambiguously permit assignment of sex to Omo I. The form of the greater sciatic notch is consistent with either sex; the acetabulum is large, which suggests a male, but a preauricular sulcus is present, which strongly suggests a female (Rogers and Saunders, 1994). On the basis of femoral morphology, including its relatively thin femoral cortex, lack of medullary stenosis, and diaphyseal shape at midshaft and the distal shaft, Kennedy (1984) noted that Omo I more closely resembled the females of a Romano-British control sample and tentatively suggested that the specimen might be female.

The morphology of the auricular surface of the os coxae suggests a young adult age. The preserved portion of the left humerus suggests that Omo I was quite tall, perhaps 178–182 cm, but the first metatarsal suggests a shorter stature of 162–173 cm. The diameter of Omo I's femoral head can be estimated from the proximodistal diameter of its left humeral head and the maximum diameter of its left acetabulum, which predict a diameter of 47.28 ± 1.24 mm. Using Grine et al.'s (1995) formula, body mass can be estimated as 70.73 ± 5.14 kg. The long, slender limbs of Omo I and its moderate estimates for body mass suggest that the individual had a linear, perhaps even Nilotic physique (Roberts and Bainbridge, 1963), in common with early *Homo erectus* and specimens such as the ~500,000-year-old Baringo ulna (Solan and Day, 1992; Deino and McBrearty, 2002), which is most probably attributable to *Homo heidelbergensis*.

Acknowledgments

We are grateful to Waizerit Mamitu Yilma, Director of the National Museum of Ethiopia and Ato Jara Haile Mariam, Director General of the Authority for Research and Conservation of Cultural Heritage (ARCCH) for access to the fossils, and to Ato Alemu Admassu, who facilitated the study of the material. We thank Dr. Solomon Yirga and Dr. Mulugeta Fesseaha for hospitality in Addis Ababa. Many people contributed to the Kibish Paleontological Project, including Dr. Zelalem Assefa, Dr. Frank Brown, Dr. Ian McDougall, Dr. Craig Feibel, Dr. John Shea, and Dr. Josh Trapani. Funding for fieldwork in Ethiopia was provided by NSF BCS-9817950 and NSF BCS-0097112, the L.S.B. Leakey Foundation, the National Geographic Society, and Australian National University. DFR's work was supported by a Social Sciences and Humanities Research Council of Canada Doctoral Fellowship. We thank Drs. Chris Stringer, Steve Churchill, Bill Kimbel, and an anonymous reviewer for their many helpful comments on an earlier draft of the manuscript.

References

Arsuaga, J.L., Carretero, J.M., 1994. Multivariate analysis of the sexual dimorphism of the hip bone in a modern human population and in early hominids. Am. J. Phys. Anthropol. 93, 241–257.
Boulle, E.-L., 2001. Osteological features associated with ankle hyperdorsiflexion. Int. J. Osteoarchaeol. 11, 345–349.
Brown, F.H., Fuller, C.R., 2008. Stratigraphy and tephra of the Kibish Formation, southwestern Ethiopia. J. Hum. Evol. 55, 366–403.
Butzer, K.W., 1969. Geological interpretation of two Pleistocene hominid sites in the Lower Omo Basin. Nature 222, 1133–1135.
Butzer, K.W., Thurber, D.L., 1969. Some late Cenozoic sedimentary formations of the Lower Omo Basin. Nature 222, 1138–1142.
Byers, S., Akoshima, K., Curran, B., 1989. Determination of adult stature from metatarsal length. Am. J. Phys. Anthropol. 79, 275–279.
Carretero, J.M., Lorenzo, C., Arsuaga, J.L., 1999. Axial and appendicular skeleton of *Homo antecessor*. J. Hum. Evol. 37, 459–499.
Churchill, S.E., Formicola, V., 1997. A case of marked bilateral asymmetry in the upper limbs of an Upper Palaeolithic male from Barma Grande (Liguria), Italy. Int. J. Osteoarchaeol. 7, 18–38.
Churchill, S.E., Pearson, O.M., Grine, F.E., Trinkaus, E., Holliday, T.W., 1996. Morphological affinities of the proximal ulna from Klasies River Mouth Main Site: archaic or modern? J. Hum. Evol. 31, 213–237.
Clark, J.D., 1988. The Middle Stone Age of East Africa and the beginnings of regional identity. J. World Prehist. 2, 235–305.
Day, M.H., 1969. Omo human skeletal remains. Nature 222, 1135–1138.
Day, M.H., 1972. The Omo human skeletal remains. In: Bordes, F. (Ed.), The Origin of *Homo sapiens*. UNESCO, Paris, pp. 31–35.
Day, M.H., Twist, M.H.C., Ward, S., 1991. Les vestiges post-crâniens d'Omo I (Kibish). L'Anthropologie 95, 595–610.
Deino, A.L., McBrearty, S., 2002. $^{40}Ar/^{39}Ar$ dating of the Kapthurin Formation, Baringo, Kenya. J. Hum. Evol. 42, 185–210.
Drapeau, M.S.M., 2004. Functional anatomy of the olecranon process in hominoids and Plio-Pleistocene hominins. Am. J. Phys. Anthropol. 124, 297–314.
Endo, B., 1971. Some characteristics of the deltoid tuberosity of the humerus in West-Asian and European "classic" Neanderthals. J. Anthropol. Soc. Japan 79, 249–258.
Endo, B., Kimura, T., 1970. Postcranial skeleton of the Amud man. In: Suzuki, H., Takai, F. (Eds.), The Amud Man and His Cave Site. Academic Press of Japan, Tokyo, pp. 231–406.
Feibel, C.S., 2008. Microstratigraphy of the Kibish hominin sites KHS and PHS, Lower Omo Valley, Ethiopia. J. Hum. Evol. 55, 404–408.
Gambier, D., 1982. Étude ostéométrique des astragles néandertaliens du Régourdou (Montignac, Dordogne). C. R. Acad. Sci. Paris Sér. II 295 297–282.
Grine, F.E., Jungers, W.L., Tobias, P.V., Pearson, O.M., 1995. Fossil *Homo* femur from Berg Aukas, northern Namibia. Am. J. Phys. Anthropol. 97, 151–185.
Hambucken, A., 1993. Révision des particularités de l'humérus des Néandertaliens Européens. C.R. Acad. Sci. Paris Sér. II 317, 109–114.
Kaufmann, H., 1941. Recherches de morphologie humaine comparative: le squelette du pied chez les Boschimans, les Hottentots, et les Griquas. Arch. Suisses d'Anthropol. Gén. 9, 195–301.
Kennedy, G.E., 1984. The emergence of *Homo sapiens*: the post cranial evidence. Man 19, 94–110.
Klein, R.G., 1999. The Human Career, second ed. University of Chicago Press, Chicago.
Leakey, R.E.F., 1969. Faunal remains from the Omo Valley. Nature 222, 1132–1133.
Martin, R., Saller, K., 1957. Lehrbuch der Anthropologie. Gustav Fischer Verlag, Stuttgart.
Matiegka, J., 1938. *Homo Předmostensis*: Fosilní Člověk z Předmostí na Moravě II. Ostatní Části Kostrové. Nákaladem České Akademie Věd e Umění, Prague.
McCown, T.D., Keith, A., 1939. The Stone Age of Mount Carmel, Vol. II: The Fossil Human Remains from the Levalloiso-Mousterian. Clarendon Press, Oxford.
McDougall, I., Brown, F.H., Fleagle, J.G., 2005. Stratigraphic placement and age of modern humans from Kibish, Ethiopia. Nature 433, 733–736.
McDougall, I., Brown, F.H., Fleagle, J.G., 2008. Sapropels and the age of hominins Omo I and II, Kibish, Ethiopia. J. Hum. Evol. 55, 409–420.
Musgrave, J.H., 1971. How dextrous was Neanderthal man? Nature 233, 538–541.
Pearson, O.M., 1997. Postcranial morphology and the origin of modern humans. Ph.D. Dissertation, State University of New York at Stony Brook.
Pearson, O.M., 2000a. Postcranial remains and the origin of modern humans. Evol. Anthropol. 9, 229–247.
Pearson, O.M., 2000b. Activity, climate, and postcranial robusticity: Implications for modern human origins and scenarios of adaptive change. Curr. Anthropol. 41, 569–607.

Pearson, O.M., Grine, F.E., 1996. Morphology of the Border Cave hominid ulna and humerus. S. Afr. J. Sci. 92, 231–236.
Pearson, O.M., Grine, F.E., 1997. Re-analysis of the hominid radii from Cave of Hearths and Klasies River Mouth, South Africa. J. Hum. Evol. 32, 577–592.
Rhoads, J.G., Trinkaus, E., 1977. Morphometrics of the Neandertal talus. Am. J. Phys. Anthropol. 46, 29–43.
Roberts, D.L., Bainbridge, D.R., 1963. Nilotic physique. Am. J. Phys. Anthropol. 21, 341–370.
Rogers, T., Saunders, S., 1994. Accuracy of sex determination using morphological traits of the human pelvis. J. Forensic Sci. 39, 1047–1056.
Smith, R.J., 1996. Biology and body size in human evolution. Curr. Anthropol. 37, 451–481.
Solan, M., Day, M.H., 1992. The Baringo (Kapthurin) ulna. J. Hum. Evol. 22, 307–313.
Steele, D.G., Bramblett, C.A., 1988. The Anatomy and Biology of the Human Skeleton. Texas A&M University Press, College Station.
Trinkaus, E., 1983. The Shanidar Neandertals. Academic Press, New York.
Trinkaus, E., Churchill, S.E., 1988. Neandertal radial tuberosity orientation. Am. J. Phys. Anthropol. 75, 15–21.
Trinkaus, E., Churchill, S.E., Ruff, C.B., 1994. Postcranial robusticity in *Homo*. II: Bilateral asymmetry and bone plasticity. Am. J. Phys. Anthropol. 93, 1–34.
Trotter, M., 1970. Estimation of stature from intact long bones. In: Stewart, T.D. (Ed.), Personal Identification in Mass Disasters. National Museum of Natural History, Washington, pp. 71–83.
Twist, M.H.C., 1985/1986. Hominid foot bones from the Kibish Formation of the Lower Omo Valley. B.Sc. Anatomy Project, Department of Anatomy, United Medical and Dental Schools of Guy's and St. Thomas' Hospitals, London.
Vandermeersch, B., 1981. Les Hommes Fossiles de Qafzeh (Israël). CNRS, Paris.
Voisin, J.-L., 2008. The Omo I hominin clavicle: Archaic or modern? J. Hum. Evol. 55, 438–443.
Vlček, E., 1975. Morphology of the first metacarpal of Neanderthal individuals from the Crimea. Bull. Mém. Soc. Anthropol. Paris, Sér. 13 2, 257–276.
Walker, A., Leakey, R., 1993. The postcranial bones. In: Walker, A., Leakey, R. (Eds.), The Nariokotome *Homo erectus* Skeleton. Harvard University Press, Cambridge, pp. 95–160.
Ward, S., 1986. Assessment of Omo I post-cranial morphology. B.Sc. Anatomy Project, Department of Anatomy, United Medical and Dental Schools of Guy's and St. Thomas' Hospitals, London.